

Original Article

Synthesis, Spectroscopic Study and Electrochemistry of Mononuclear Copper (II)-Bis-Azide-Naphthyl-Azo-Imidazole/Benzimidazole/Pyridine and Binuclear Copper(II)-Azide-Bridged-Naphthyl-Azo-Imidazole/Benzimidazole/Pyridine Complexes

Prithwiraj Byabartta* and Somnath Sau

Department of Chemistry, Jogesh Chandra Chaudhuri College, 30- Prince Anwar Shah Road, Kolkata, India

ARTICLE INFO

Corresponding Author:

Prithwiraj Byabartta
pribatta@gmail.com

How to cite this article:

Byabartta, P., and S. Sau. 2014. Synthesis, Spectroscopic Study and Electrochemistry of Mononuclear Copper (II)-Bis-Azide-Naphthyl-Azo-Imidazole/Benzimidazole/Pyridine and Binuclear Copper (II)-Azide-Bridged-Naphthyl-Azo-Imidazole/Benzimidazole/Pyridine Complexes. *The Journal of Applied Sciences Research*. 1(4): 284-305.

Article History:

Received: 12 December 2014
Accepted: 28 December 2014

ABSTRACT

Reaction of copper perchlorate hexahydrate $[\text{Cu}(\text{H}_2\text{O})_6](\text{ClO}_4)_2$ with NaaiR' in Acetone medium following ligand addition leads to $[\text{Cu}(\text{N}_3)_2(\text{NaaiR}')_2]$ and $[\text{Cu}_2(\text{--N}_3)_2(\text{NaaiR}')_2]$, $\text{NaaiR}' = \text{naphthyl-azo-imidazole/benzimidazole/pyridine} = \text{C}_{10}\text{H}_4\text{-N=N-} / \text{C}_3\text{H}_2\text{-NN-1-R}'$, (R' imidazole) / $\text{C}_7\text{H}_4\text{-NN-1-H}$ (Benzimidazole), / $\text{C}_3\text{H}_4\text{-N-}$ (Pyridine), abbreviated as N,N'-chelator, where N(imidazole) and N(azo) represent N and N', respectively; R' = H(a), Me (b), N₃ = monodentate azide linkage, --N₃ = azide bridged binuclear complex]. The ¹H NMR spectral measurements suggest the molecular structure of bis chelated complex with the protons at the aromatic region and naphthyl protons at higher value. The voltammogram also shows a small anodic peak at 0.2 V, possibly due to the Cu (I)/Cu (0) couple.

Keywords: Copper (II), azide, binuclear, Naphthylazoimidazole, CV, NMR, IR, ESIMS.

Copyright © 2014, World Science and Research Publishing. All rights reserved.

INTRODUCTION

The copper complex had presumably square-pyramidal coordination geometry, with an additional thioether group attached to the central N atom in the axial position. The anti-proliferative activity screening revealed that was endowed with the lowest inhibitory effect, indicating that an additional substituent on the central nitrogen was necessary for eliciting cytotoxic activity. The authors speculated that the nearly planar arrangement of the two

benzimidazole units and the cupric ion was not a requirement for biological activity. Interestingly, and had a significant inhibitory effect on K562 cancer cells compared to the low toxicity exhibited against healthy bone marrow cells (Prithwiraj *et al.*, 2001; Byabartta *et al.*, 2003; Avudoddi *et al.*, 2014; Ki-Joong *et al.*, 2014; Xin *et al.*, 2014; Rangasamy *et al.*, 2014; Kai *et al.*, 2014; Giulia, Qian *et al.*, 2014; Yan-Fu *et al.*, 2014; Daniel Mendoza *et al.*, 2014; Noriaki *et al.*, 2014; Antonino, Riccardo *et al.*, 2014). The synthesis and structures of two copper(II) complexes with a benzothiazole sulfonamide ligand, [Cu((py), and [Cu((en) (-2-(4-methylbenzothiazole) toluenesulfonamide, py = pyridine, en = ethylenediamine), were described, exhibit eda square-planar geometry, and displayed a distorted octahedral array, showed different coordination modes: through the benzothiazole N in and through the sulfonamide N in. The ability of the complexes to cleave CT-DNA was studied in vitro through ascorbate activation and tested by monitoring expression of the yEGFP gene containing the RAD54 reporter. Both were found to cleave DNA in vitro, and were found to be more effective in inhibiting Caco-2 and Jurkat T cell growth. There are several copper (II) compounds involving a 1, 2, 4-triazole moiety (Triazoles, Tetrazoles, and Oxazoles) that show a wide range of biological and pharmacological activities. The Cu (II) complex [Cu()Cl emerged from a number of triazolemetal-based compounds] screened for their cytotoxicity in human cancer cells. It was found that, by inhibiting caspase-3, impaired execution of the apoptotic program, thus addressing the cells to alternative death pathways, such as paraptosis. Gene expression profiling of the human fibrosarcoma. HT1080 cells showed that upregulated genes involved in the unfolded protein response (UPR) and response to heavy metals. The variety of metal ion functions in biology has stimulated the development of new metallo-drugs other than Pt drugs with the aim to obtain compounds acting via alternative mechanisms of action. Among non-Pt compounds, copper complexes are potentially attractive as anticancer agents. Actually, since many years a lot of researches have actively investigated copper compounds based on the assumption proposal that endogenous metals may be less toxic.

It has been established that the properties of copper-coordinated compounds are largely determined by the nature of ligands and donor atoms bound to the metal ion. In this review, the most remarkable achievements in the design and development of copper(I, II) complexes as antitumor agents are discussed (Yang Fei *et al.*, 2014; Syuzanna *et al.*, 2014; Harshita *et al.*, 2014; Showmya *et al.*, 2014; Leung King Pong, Chen Dongshi *et al.*, 2014; Kim Sang-Min, Kim Jae-Hyun *et al.*, 2014; Cadot Stéphane *et al.*, 2014; Papaefstathiou *et al.*, 2014; Baiju *et al.*, 2014; Lianchao *et al.*, 2014; Iman *et al.*, 2014; Musacco *et al.*, 2014; Shuang *et al.*, 2014; Hao *et al.*, 2014; Mahboobeh *et al.*, 2014; Zuofeng *et al.*, 2014; Zhi-Kun *et al.*, 2014). Special emphasis has been focused on the identification of structure-activity relationships for the different classes of copper (I, II) complexes. This work was motivated by the observation that no comprehensive surveys of copper complexes as anticancer agents were available in the literature. Moreover, up to now, despite the enormous efforts in synthesizing different classes of copper complexes, very few data concerning the molecular basis of the mechanisms underlying their antitumor activity are available. Copper (II) and copper (I)-diimine complexes (diimine function) have attracted much research interest in the realm of science and technology. Cu (II) prefers distorted octahedral (six coordinate), square pyramidal (five coordinate) or square planar (tetra coordinate) while Cu (I) demands, in general, tetrahedral geometry. The redox change Cu(II), Cu(I) or vice versa is associated with structural change which requires large reorganization energy (Pinxian *et al.*, 2014; Hang *et al.*, 2014; Xin and Guosheng, 2014; Zikun *et al.*, 2014; Benjamin *et al.*, 2014; Shusen *et al.*, 2014; Luke *et al.*, 2014; Alice Kay *et al.*, 2014; Chen *et al.*, 2014; Tadeu Santiago *et al.*, 2014; Alexandre *et al.*, 2014; Pangkita, 2014; Anna, Machura Barbara *et al.*, 2014, Li Shengliang *et al.*, 2014; Jae-Hoon *et al.*, 2014; Suchand *et al.*, 2014; Kommuri *et al.*, 2014; Venkata *et al.*, 2014; Youngmi *et al.*, 2014; Fernando *et al.*, 2014). In fact this energy has been utilized by biochemical processes. Thio ether donors destabilize Cu (II) state elevating

the Cu (II), Cu(I) redox potentials which includes structural flexibility in the stabilization of Cu(I) state. The electronic property of thio ether containing ligands may be controlled by incorporating substituents in the conjugated framework of the ligand system. Incorporation of photochromic molecules into organic or hybrid organic–inorganic materials leads to the development of very effective devices for optical data recording and storage. Azo-conjugated metal complexes exhibit unique properties upon light irradiation in the area of photon-mode high-density information storage photoswitching devices (Yuwen *et al.*, 2014; Yifeng and Haiyan, 2014; Dantas *et al.*, 2014; Zonghao *et al.*, 2014; Nahid and Golmohammadi, 2014, Christopher and Johnston, 2014; Jonathan *et al.*, 2014; Shu-Hao *et al.*, 2014; Wen *et al.*, 2014; Wei *et al.*, 2014; Fei, 2014; Huijie *et al.*, 2014; Fairbairn *et al.*, 2014; Khemnar and Bhanage, 2014; Roberto *et al.*, 2014; Masako *et al.*, 2014; Hongxia *et al.*, 2014; Christopher *et al.*, 2012). The proposed curative properties of Cu-based non-steroidal anti-inflammatory drugs (NSAIDs) have led to the development of numerous Cu (II) complexes of NSAIDs with enhanced anti-inflammatory activity and reduced gastrointestinal (GI) toxicity compared with their uncomplexed parent drug. These low toxicity Cu drugs have yet to reach an extended human market, but are of enormous interest, because many of today's anti-inflammatory drug therapies, including those based on the NSAIDs, remain either largely inadequate and/or are associated with problematic renal, GI and cardiovascular side effects. The origins of the anti-inflammatory and gastric-sparing actions of Cu-NSAIDs, however, remain uncertain. Their ability to influence copper metabolism has been a matter of debate and, apart from their frequently reported superoxide dismutase (SOD)-like activity *in vitro*, relatively little is known about how they ultimately regulate the inflammatory process and/or immune system. Furthermore, little is known of their pharmacokinetic and biodistribution profile in both humans and animals, stability in biological media and pharmaceutical formulations, or the relative potency/efficacy of the Cu (II) monomeric versus Cu (II) dimeric complexes. It will also compare the SOD, anti-inflammatory and ulcerogenic effects of various Cu-NSAIDs. If the potential opportunities of the Cu-NSAIDs are to be completely realized, a mechanistic understanding and delineation of their *in vivo* and *in vitro* pharmacological activity is fundamental, along with further characterization of their pharmacokinetic/pharmacodynamic disposition. Elesclomol (N1 dimethyl-N,-di(phenylcarbonothio-yl) malonohydrazide, 1) is a novel small molecule anticancer drug candidate that is discovered and originated from our lab. It exhibits strong antitumor activities against a broad range of cancer cell lines including MDR (multi-drug resistance) cell lines. It is believed that elesclomol exerts its anticancer activity via the induction of reactive oxygen species (ROS) in cancer cells, which results in apoptosis. Recent biological data support the hypothesis that elesclomol generates ROS via its chelation with copper (II) and redox cycling of copper(II). The data suggest that elesclomol obtains copper (II) outside the cell –from serum as well as from purified ceruloplasmin the primary copper-binding protein in blood–and requires copper(II) for its cellular entry and cytotoxicity. On the other hand, copper(II) complexes are of continuing interest for their potential applications as molecular imaging agents (Alexey *et al.*, 2012, Pampa *et al.*, 2012, Rathinasabapathi *et al.*, 2012, Kozlev ar Bojan, Kitanovski Nives *et al.*, 2012, Comba Peter, Haaf Christina *et al.*, 2012; Xiaolin *et al.*, 2012, Osório *et al.*, 2012, Nagy Nóra *et al.*, 2012, Reger Daniel L., Debreczeni Agota *et al.*, 2011; Linda *et al.*, 2012). They were investigated as anticancer agents for their capability to induce the formation of ROS and to inhibit proteasome activities in cancer cells. Recent publications on elesclomol prompt us to communicate our earlier results in the synthesis, crystallographic characterization, and the electrochemical property measurements of the elesclomol copper (II) complex. A series of copper(II) complexes with 2-methylbenzimidazole, 2-phenylbenzimidazole, 2-chlorobenzimidazol, 2-benzimidazolecarbamate, and 2-guanidinobenzimidazole was prepared, and their cytotoxic activity was evaluated against PC3, MCF-7, HCT-15, HeLa, SKLU-1, and U373 cancer cell lines, showing that [Cu(2-chlorobenzimidazole)Br] and [Cu(2-benzimidazolecarbamate)Br] had significant cytotoxic activity (Mendola *et al.*, 2012, Sabrina *et al.*, 2012, Gernot *et al.*,

2011, Apurba *et al.*, 2011 Kayla *et al.*, 2011, Crestani *et al.*, 2011, Murphy *et al.*, 2011, Pratik *et al.*, 2011; Sethu *et al.*, 2011; Rémi *et al.*, 2011). These results showed that the cytotoxic activity was related to the easy displacement of halides from the coordination sphere of the metal. The copper complexes, of 2-methyl-1H-benzimidazole-5-carbohydrazide and 2-methyl-N-(propan-2-ylidene)-1H-benzimidazole-5-carbohydrazide displayed cytotoxicity against A549 (ICM) tumor cell lines. A series of copper(II) complexes of tri- or tetra-dentate bis(2-methylbenzimidazolyl) amine ligands (has been prepared and fully characterized in solution as well as in the solid state. All ligands acted as tridentate donors toward the cupric ions through one central amine and two benzimidazole N atoms in the solid state. The complex [Cu (a square-pyramidal coordination water ligand and a bridging perchlorate group defined the distorted octahedral environments of complex (Fei *et al.*, 2014; *et al.*, 2014; Harshita *et al.*, 2014; Showmya *et al.*, 2014; King Pong, *et al.*, 2014; Sang-Min *et al.*, 2014; Stéphane *et al.*, 2014; Giannis *et al.*, 2014; Baiju *et al.*, 2014; Lianchao *et al.*, 2014; Iman *et al.*, 2014; Rosario Musacco *et al.*, 2014; Xu jiao shuang *et al.*, 2014; Hao *et al.*, 2014; Nasr-Esfahani *et al.*, 2014; Zuofeng *et al.*, 2014; Qu Zhi-Kun *et al.*, 2014). The cytotoxic effects of the complexes were associated with inhibition of the ubiquitin-proteasome system and accumulation of ubiquitinated proteins in a manner dependent on protein synthesis. The occurrence of the UPR during the induced death process was shown by the increased abundance of spliced XBP1 mRNA, transient eIF2 phosphorylation, and a series of downstream events, including attenuation of global protein synthesis and increased expression of ATF4, CHOP, BIP, and GADD34. Synthesized two novel chloro-bridged and bromo-bridged 1,2,4-triazole e-based Cu(II) complexes, [Cu= 3,5-bis{[bis(2-methoxyethyl)-amino]methyl}-4H-1,2,4-triazol-4-amine)]. The apparent CT-DNA binding constant (for complexes, respectively). Furthermore, both compounds displayed efficient oxidative cleavage of supercoiled DNA in the presence of external activating agents. Coordination of monodentate 5-amino-2-tert-butyltetrazole via the endo cyclic N4 atom to the Cu(II) ion produced the five-coordinated [Cu(Cl)] complex end owed with low cytotoxic activity against HeLa cells. Analogously, the octahedral copper (II) complex of 3,5-bis(2-pyridyl)-1,2,4-oxadiazole showed moderate cytotoxicity against HepG2 and HT29 cells. Cell morphological changes were observed by light microscopy, and an apoptotic death was proposed. The interaction of the cationic species with native DNA indicated that the copper complex was a DNA groove binder with binding constant.

MATERIALS AND METHOD

Material and Instrumentation

Published methods were used to prepare Naphthyl-azo-imidazole /benzimidazole/ pyridine (Prithwiraj *et al.*, 2014; Prithwiraj, 2014; Prithwiraj, 2014; Byabartta *et al.*, 2001, Byabartta *et al.*, 2003, Avudoddi *et al.*, 2014; Ki-Joong *et al.*, 2014; Huang Xin *et al.*, 2014; Rangasamy *et al.*, 2014; Kang Kai *et al.*, 2014; Sapuppo Giulia *et al.*, 2014; Yan-Fu *et al.*, 2014; Mendoza *et al.*, 2014; Noriaki *et al.*, 2014; Antonino *et al.*, 2014). All other chemicals and organic solvents used for preparative work were of reagent grade (SRL, Sigma Alhrich). Microanalytical data (C, H, N) were collected using a Perkin Elmer 2400 CHN instrument. I.r. spectra were obtained using a JASCO 420 spectrophotometer (using KBr disks, 4000-200 cm^{-1}). The ^1H nmr spectra in CDCl_3 were obtained on a Bruker 500 MHz FT n.m.r spectrometer using SiMe_4 as internal reference, CFCl_3 (external ^{19}F). Solution electrical conductivities were measured using a Systronics 304 conductivity meter with solute concentration $\sim 10^{-3}$ M in acetonitrile. Mass spectra were recorded on VG Autospec ESI-mass spectrometry. Electrochemical work was carried out using an EG & G PARC Versastat computer controlled 250 electrochemical system. All experiments were performed under a N_2 atmosphere at 298K using a Pt-disk milli working electrode at a scan rate of 50 mVs^{-1} . All results were referenced to a saturated calomel electrode (SCE).

Preparation of the Complexes

Synthesis of the compound 1: PAIm(0.16g =0.00093 mole) +CuCl₂ (0.1585g =1eqv) +NaN₃(0.07g), Solvent use –Acetone/sharp colour change was observed. 16g i.e 0.00093mole PAIm was dissolved in acetone solvent 0.1585gof CuCl₂ i.e 1 equivalent was added into this solution. Now 0.07g i.e1 eqv of NaN₃ was added into the mixture and the colour change was observed. The whole mixture was stirred for 12 hours. After the completion of the reaction it was filtered & filtrate was collected for crystal tube setting and for another characterization analysis of the compound.

Characterisation of the Compound 1: CHN calculation of the above compound [C₁₈H₁₆N₁₄Cu₂], gives Calc(found): C, 38.91(38.9), H, 2.90 (2.9), N, 35.30(35.3); IR Spectroscopic data, ν (N=N) 1370 ν (C=N) 1590, ESI/MS Spectroscopic data, 555.5 [M⁺], Proton n.m.r. Spectroscopic data, ¹H, ppm, 8.07(d, J = 8Hz, H(7,11)), 8.01(d, J=6.5Hz, H(8,10)), 7.09(m, 9-H), 7.26(d, J=6Hz, H(4)), 7.34(d, J=5Hz, H(5)), 1.5(s, N-Me); UV-Vis Spectroscopic data, (nm), 280(8160), 382(8200), 595(600),(sh); Electrochemistry or Cyclic Voltammetric data (E_{1/2} (V) (E_p(mV) [Solvent MeCN, Supporting Electrolyte, Bu₄NClO₄ (0.1 M), scan rate 50 mVs⁻¹, Pt disk working electrode, Pt wire auxiliary electrode, reference electrode SCE at 298 K] ligand reduction -0.63 (110);

Synthesis of the Compound 2. PAIm(0.3285 =0.00191 mole) + CuCl₂ (0.3256g=1eqv) +NaN₃ (0.2483g=2eqv), Solvent use –Acetone/sharp colour change was observed. 0.3285g i.e 0.00191mole PAIm was dissolved in acetone solvent 0.3256gof CuCl₂ i.e 1 equivalent was added into this solution. Now 0.2483g i.e2 eqv of NaN₃ was added into the mixture and the colour change was observed. The whole mixture was stirred for 12 hours. After the completion of the reaction it was filtered & filtrate was collected for crystal tube setting and for another charecterisation analysis of the compound.

Characterisation of the Compound 2: CHN calculation of the above compound [C₉H₈N₁₀Cu₁], gives Calc(found): C, 33.80(33.8), H 2.52 (2.6), N, 43.80(43.8); IR Spectroscopic data, ν (N=N) 1370 ν (C=N) 1590, ESI/MS Spectroscopic data, 319.76 [M⁺], Proton n.m.r.Spectroscopic data, ¹H, ppm, 8.07(d, J = 8Hz, H(7,11)), 8.01(d, J=6.5Hz, H(8,10)), 7.09(m, 9-H), 7.26(d, J=6Hz, H(4)), 7.34(d, J=5Hz, H(5)), 1.5(s, N-Me); UV-Vis Spectroscopic data, (nm), 244(10500), 280(8160), 282(8200), 295(600),(sh); Electrochemistry or Cyclic Voltammetric data (E_{1/2} (V) (E_p(mV) [Solvent MeCN, Supporting Electrolyte, Bu₄NClO₄ (0.1 M), scan rate 50 mVs⁻¹, Pt disk working electrode, Pt wire auxiliary electrode, reference electrode SCE at 298 K] ligand reduction -0.56 (100).

Synthesis of the Compound 3. NAIIm (0.0529g =0.00024 mole) +CuCl₂ (0.04092g=1eqv) + NaN₃(0.0156g=1eqv), Solvent use –Acetone / sharp colour change was observed .0529g i.e 0.00024 mole NAIIm was dissolved in acetone solvent .04092 g of CuCl₂ i.e 1 equivalent was added into this solution. Now 0.0156g i.e 1 eqv of NaN₃ was added into the mixture and the colour change was observed. The whole mixture was stirred for 12 hours.after the completion of the reaction it was filtered & filtrate was collected for crystal tube setting and for another charecterisation analysis of the compound.

Characterisation of the compound 3: CHN calculation of the above compound [C₂₆H₂₀N₁₄Cu₂], gives Calc(found): C, 47.63 (47.7), H, 3.07 (3.1), N, 29.90(29.9); IR Spectroscopic data, ν (N=N) 1372 ν (C=N) 1594, ESI/MS Spectroscopic data, 655.6 [M⁺], Proton n.m.r.Spectroscopic data, ¹H, ppm, 8.01(d, J = 8Hz, H(7,11)), 8.11(d, J=6.5Hz, H(8,10)), 7.09(m, 9-H), 7.26(d, J=6Hz, H(4)), 7.34(d, J=5Hz, H(5)), 1.5(s, N-Me); UV-Vis Spectroscopic data, (nm), 280(10160), 382(8200), 545(900),(sh); Electrochemistry or Cyclic Voltammetric data (E_{1/2} (V) (E_p(mV) [Solvent MeCN, Supporting Electrolyte,

Bu₄NClO₄ (0.1 M), scan rate 50 mVs⁻¹, Pt disk working electrode, Pt wire auxiliary electrode, reference electrode SCE at 298 K] ligand reduction -0.52 (100);

Synthesis of the Compound 4: NAIM(0.1002g =0.00045 mole) + CuCl₂ (0.07672g=1eqv) + NaN₃(0.05851g=2eqv), Solvent use –Acetone/sharp colour change was observed. 1002g i.e 0.00045 mole NAIM was dissolved in acetone solvent .07672 g of CuCl₂ i.e 1 equivalent was added into this solution. Now 0.05851g i.e2 eqv of NaN₃ was added into the mixture and the colour change was observed. The whole mixture was stirred for 12 hours.after the completion of the reaction it was filtered & filtrate was collected for crystal tube setting and for another charecterisation analysis of the compound.

Characterisation of the Compound 4: CHN calculation of the above compound [C₁₃H₁₀N₁₀Cu₁], gives Calc(found): C, 42.21 (42.3), H, 2.72 (2.8), N, 37.87(37.9); IR Spectroscopic data, ν (N=N) 1373 ν (C=N) 1593, ESI/MS Spectroscopic data, 369.8 [M⁺], Proton n.m.r. Spectroscopic data, ¹H, ppm, 8.00(d, J = 8Hz, H(7,11)), 8.09(d, J=6.5Hz, H(8,10)), 7.19(m, 9-H), 7.36(d, J=6Hz, H(4)), 7.44(d, J=5Hz, H(5)); UV-Vis Spectroscopic data, (nm), 244(10500), 282(8200), 295(600),(sh); Electrochemistry or Cyclic Voltammetric data (E_{1/2} (V) (E_p(mV) [Solvent MeCN, Supporting Electrolyte, Bu₄NClO₄ (0.1 M), scan rate 50 mVs⁻¹, Pt disk working electrode, Pt wire auxiliary electrode, reference electrode SCE at 298 K] ligand reduction -0.55 (106);

Synthesis of the Compound 5. MeNAIm(0.0545g =0.00023 mole) + CuCl₂ (0.03921g=1eqv) + NaN₃(0.01495g=1eqv), Solvent use –Acetone/sharp colour change was observed. 0545g i.e 0.00023 mole NAIM was dissolved in acetone solvent 0.03921 g of CuCl₂ i.e 1 equivalent was added into this solution. Now 0.01495g i.e 1 eqv of NaN₃ was added into the mixture and the colour change was observed. The whole mixture was stirred for 12 hours. After the completion of the reaction it was filtered & filtrate was collected for crystal tube setting and for another charecterisation analysis of the compound.

Characterisation of the Compound 5: CHN calculation of the above compound [C₂₈H₂₄N₁₄Cu₂], gives Calc(found): C 49.18 (49.2), H, 3.53 (3.5), N, 28.68(28.7); IR Spectroscopic data, ν (N=N) 1373 ν (C=N) 1596, ESI/MS Spectroscopic data,683.6 [M⁺], Proton n.m.r.Spectroscopic data, ¹H, ppm, 8.0(d, J = 8Hz, H(7,11)), 8.1(d, J=6.5Hz, H(8,10)), 7.9(m, 9-H), 7.6(d, J=6Hz, H(4)), 7.34(d, J=5Hz, H(5)); UV-Vis Spectroscopic data, (nm), 244(10500), 280(9160), 388(8200), 533(630),(sh); Electrochemistry or Cyclic Voltammetric data (E_{1/2} (V) (E_p(mV) [Solvent MeCN, Supporting Electrolyte, Bu₄NClO₄ (0.1 M), scan rate 50 mVs⁻¹, Pt disk working electrode, Pt wire auxiliary electrode, reference electrode SCE at 298 K] ligand reduction -0.6 (90);

Synthesis of the Compound 6: MeNAIm (0.0440g =0.00019 mole) + CuCl₂ (0.0323g=1eqv) + NaN₃(0.0247g=2eqv), Solvent use –Acetone/sharp colour change was observed. 0440g i.e 0.00019 moleMe- NAIM was dissolved in acetone solvent .0323g of CuCl₂ i.e 1 equivalent was added into this solution.now0.0247 i.e2 eqv of NaN₃ was added into the mixture and the colour change was observed. The whole mixture was stirred for 12 hours. After the completion of the reaction it was filtered & filtrate was collected for crystal tube setting and for another charecterisation analysis of the compound.

Characterisation of the Compound 6: CHN calculation of the above compound [C₁₄H₁₂N₁₀Cu₁], gives Calc(found): C, 42.46 (42.5), H, 6.10 (6.1), N, 35.37(35.4); IR Spectroscopic data, ν (N=N) 1371 ν (C=N) 1593, ESI/MS Spectroscopic data, 395.95 [M⁺], Proton n.m.r.Spectroscopic data, ¹H, ppm, 8.0 (d, J = 8Hz, H(7,11)), 8.03(d, J=6.5Hz, H(8,10)), 7.19(m, 9-H); UV-Vis Spectroscopic data, (nm), 244(10500), 289(8160),

299(600),(sh); Electrochemistry or Cyclic Voltammetric data ($E_{1/2}$ (V) (E_p (mV) [Solvent MeCN, Supporting Electrolyte, Bu_4NClO_4 (0.1 M), scan rate 50 mVs^{-1} , Pt disk working electrode, Pt wire auxiliary electrode, reference electrode SCE at 298 K] ligand reduction - 0.58(80).

Synthesis of the Compound 7: PABEN(0.2153g =0.00074 mole) + $CuCl_2$ (0.1653g=1eqv) + NaN_3 (0.0630g=1eqv), Solvent use –Acetone/sharp colour change was observed. 0.2153 i.e 0.00074 mole PABEN was dissolved in acetone solvent .0.1653g of $CuCl_2$ i.e 1 equivalent was added into this solution. Now .0630g i.e 1 eqv of NaN_3 was added into the mixture and the colour change was observed. The whole mixture was stirred for 12 hours.after the completion of the reaction it was filtered & filtrate was collected for crystal tube setting and for another charecterisation analysis of the compound.

Characterisation of the Compound 7: CHN calculation of the above compound [$C_{26}H_{20}N_{14}Cu_2$], gives Calc(found): C, 47.63 (47.7), H, 3.07 (3.1), N, 29.90(29.9); IR Spectroscopic data, $\nu(N=N)$ 1378 $\nu(C=N)$ 1598, ESI/MS Spectroscopic data, 312.27 [M^+], Proton n.m.r.Spectroscopic data, 1H , ppm, 8.08(d, J = 8Hz, H(7,11)), 8.03(d, J=6.5Hz, H(8,10)), UV-Vis Spectroscopic data, (nm), 288(11500), 382(9200), 544(699),(sh); Electrochemistry or Cyclic Voltammetric data ($E_{1/2}$ (V) (E_p (mV) [Solvent MeCN, Supporting Electrolyte, Bu_4NClO_4 (0.1 M), scan rate 50 mVs^{-1} , Pt disk working electrode, Pt wire auxiliary electrode, reference electrode SCE at 298 K] ligand reduction -0.52 (80).

Synthesis of the Compound 8 : PABEN(0.1444g =0.00074 mole) + $CuCl_2$ (0.1261g=1eqv) + NaN_3 (0.0962g=2eqv), Solvent use –Acetone/sharp colour change was observed. 1444g i.e 0.00074 mole PABEN was dissolved in acetone solvent .0.1261 g of $CuCl_2$ i.e 1 equivalent was added into this solution. Now 0.0962 i.e 2 eqv. of NaN_3 was added into the mixture and the colour change was observed. The whole mixture was stirred for 12 hours. After the completion of the reaction it was filtered & filtrate was collected for crystal tube setting and for another charecterisation analysis of the compound.

Characterisation of the Compound 8: CHN calculation of the above compound [$C_{13}H_{10}N_{10}Cu_1$], gives Calc(found): C, 42.21 (42.2), H, 2.72 (2.8), N, 37.87(37.9); IR Spectroscopic data, $\nu(N=N)$ 1373 $\nu(C=N)$ 1597, ESI/MS Spectroscopic data, 369.83 [M^+], Proton n.m.r.Spectroscopic data, 1H , ppm, 8.7(d, J = 8Hz, H(7,11)), 8.1(d, J=6.5Hz, H(8,10)), 7.9(m, 9-H), 7.16(d, J=6Hz, H(4)); UV-Vis Spectroscopic data, (nm), 280(8160), 282(8200), 295(600),(sh); Electrochemistry or Cyclic Voltammetric data ($E_{1/2}$ (V) (E_p (mV) [Solvent MeCN, Supporting Electrolyte, Bu_4NClO_4 (0.1 M), scan rate 50 mVs^{-1} , Pt disk working electrode, Pt wire auxiliary electrode, reference electrode SCE at 298 K] ligand reduction -0.51 (90).

Synthesis of the compound 9: MePAIm(0.0829 =0.00045 mole) + $CuCl_2$ (0.0767g=1eqv) + NaN_3 (0.0292g=1eqv), Solvent use –Acetone/sharp colour change was observed. 0829g i.e 0.00045 moleMEPAIm was dissolved in acetone solvent 0.0767 g of $CuCl_2$ i.e 1 equivalent was added into this solution. Now 0.0292g i.e 1 eqv of NaN_3 was added into the mixture and the colour change was observed. The whole mixture was stirred for 12 hours. After the completion of the reaction it was filtered & filtrate was collected for crystal tube setting and for another charecterisation analysis of the compound.

Characterisation of the Compound 9: CHN calculation of the above compound [$C_{26}H_{20}N_{14}Cu_2$], gives Calc(found): C, 41.16 (41.2), H, 3.45 (3.4), N, 33.60 (33.6); IR Spectroscopic data, $\nu(N=N)$ 1374 $\nu(C=N)$ 1593, ESI/MS Spectroscopic data, 583.5 [M^+], Proton n.m.r.Spectroscopic data, 1H , ppm, 8.7(d, J = 8Hz, H(7,11)), 8.1(d, J=6.5Hz, H(8,10)),

7.9(m, 9-H), 7.6(d, J=6Hz, H(4)), 7.4(d, J=5Hz, H(5)); UV-Vis Spectroscopic data, (nm), 280(12160), 389(10200), 533(633),(sh); Electrochemistry or Cyclic Voltammetric data ($E_{1/2}$ (V) (E_p (mV) [Solvent MeCN, Supporting Electrolyte, Bu_4NClO_4 (0.1 M), scan rate 50 mVs^{-1} , Pt disk working electrode, Pt wire auxiliary electrode, reference electrode SCE at 298 K] ligand reduction -0.5 (90).

Synthesis of the Compound 10: MePAIm(0.1920 =0.00103 mole) + $CuCl_2$ (0.1755g=1eqv) + NaN_3 (0.1339g=2eqv), Solvent use –Acetone/sharp colour change was observed. 1920g i.e 0.00103 mole MEPAIm was dissolved in acetone solvent .0.1755 g of $CuCl_2$ i.e 1 equivalent was added into this solution. Now 0.1339g i.e2 eqv of NaN_3 was added into the mixture and the colour change was observed. The whole mixture was stirred for 12 hours. After the completion of the reaction it was filtered & filtrate was collected for crystal tube setting and for another charecterisation analysis of the compound.

Characterisation of the Compound 10: CHN calculation of the above compound [$C_{10}H_{10}N_{10}Cu_1$], gives Calc(found): C, 35.98 (35.9), H, 3.01 (3.00), N, 41.96(41.9); IR Spectroscopic data, $\nu(N=N)$ 1371 $\nu(C=N)$ 1595, ESI/MS Spectroscopic data, 333.79 [M^+], Proton n.m.r.Spectroscopic data, 1H , ppm, 8.7(d, J = 8Hz, H(7,11)), 8.1(d, J=6.5Hz, H(8,10)), 7.9(m, 9-H), 7.6(d, J=6Hz, H(4)), 7.4(d, J=5Hz, H(5)), UV-Vis Spectroscopic data, (nm), 280(7760), 282(8660); Electrochemistry or Cyclic Voltammetric data ($E_{1/2}$ (V) (E_p (mV) [Solvent MeCN, Supporting Electrolyte, Bu_4NClO_4 (0.1 M), scan rate 50 mVs^{-1} , Pt disk working electrode, Pt wire auxiliary electrode, reference electrode SCE at 298 K] ligand reduction -0.6 (100);

Synthesis of the compound 11: NABEN (0.0134g =0.00005mole) + $CuCl_2$ (0.0085g=1eqv) + NaN_3 (0.0065g=2eqv), Solvent use –Acetone/sharp colour change was observed. 0134g i.e 0.00005 mole NABEN was dissolved in acetone solvent. 0.0085g of $CuCl_2$ i.e 1 equivalent was added into this solution. Now 0.0065g i.e2 eqv of NaN_3 was added into the mixture and the colour change was observed. The whole mixture was stirred for 12 hours. After the completion of the reaction it was filtered & filtrate was collected for crystal tube setting and for another charecterisation analysis of the compound.

Characterisation of the Compound 11: CHN calculation of the above compound [$C_{10}H_{10}N_{10}Cu_1$], gives Calc(found): C, 48.62 (48.6), H, 2.88 (2.8), N, 33.35(33.5); IR Spectroscopic data, $\nu(N=N)$ 1376 $\nu(C=N)$ 1596, ESI/MS Spectroscopic data, 419.8 [M^+], Proton n.m.r.Spectroscopic data, 1H , ppm, 8.00(d, J = 8Hz, H(7,11)), 8.01(d, J=6.5Hz, H(8,10)), 7.09(m, 9-H), 7.26(d, J=6Hz, H(4)), 7.34(d, J=5Hz, H(5)), UV-Vis Spectroscopic data, (nm), 284(10500), 380(8160), 562(800); Electrochemistry or Cyclic Voltammetric data ($E_{1/2}$ (V) (E_p (mV) [Solvent MeCN, Supporting Electrolyte, Bu_4NClO_4 (0.1 M), scan rate 50 mVs^{-1} , Pt disk working electrode, Pt wire auxiliary electrode, reference electrode SCE at 298 K] ligand reduction -0.6 (90).

Synthesis of the Compound 12: PABEN(0.1444g =0.00074 mole) + $CuCl_2$ (0.1261g=1eqv) + NaN_3 (0.0962g=2eqv), Solvent use –Acetone/sharp colour change was observed. 1444g i.e 0.00074 mole PABEN was dissolved in acetone solvent .0.1261g of $CuCl_2$ i.e 1 equivalent was added into this solution. Now 0.0962g i.e2 eqv of NaN_3 was added into the mixture and the colour change was observed. The whole mixture was stirred for 12 hours. After the completion of the reaction it was filtered & filtrate was collected for crystal tube setting and for another charecterisation analysis of the compound.

Characterisation of the Compound 12: CHN calculation of the above compound [$C_{12}H_{10}N_{10}Cu_1$], gives Calc(found): C, 48.62 (48.6), H, 2.88 (2.8), N, 33.35(33.5); IR

Spectroscopic data, $\nu(\text{N}=\text{N})$ 1378 $\nu(\text{C}=\text{N})$ 1598, ESI/MS Spectroscopic data, 369.8 $[\text{M}^+]$, Proton n.m.r.Spectroscopic data, ^1H , ppm, 8.07(d, $J = 8\text{Hz}$, H(7,11)), 8.01(d, $J=6.5\text{Hz}$, H(8,10)), 7.09(m, 9-H), 7.26(d, $J=6\text{Hz}$, H(4)), 7.34(d, $J=5\text{Hz}$, H(5)), 1.5(s, N-Me); UV-Vis Spectroscopic data, (nm), 244(10500), 280(8160), 282(8200), 295(600),(sh); Electrochemistry or Cyclic Voltammetric data ($E_{1/2}$ (V) (E_p (mV) [Solvent MeCN, Supporting Electrolyte, Bu_4NClO_4 (0.1 M), scan rate 50 mVs^{-1} , Pt disk working electrode, Pt wire auxiliary electrode, reference electrode SCE at 298 K] ligand reduction -0.56 (100).

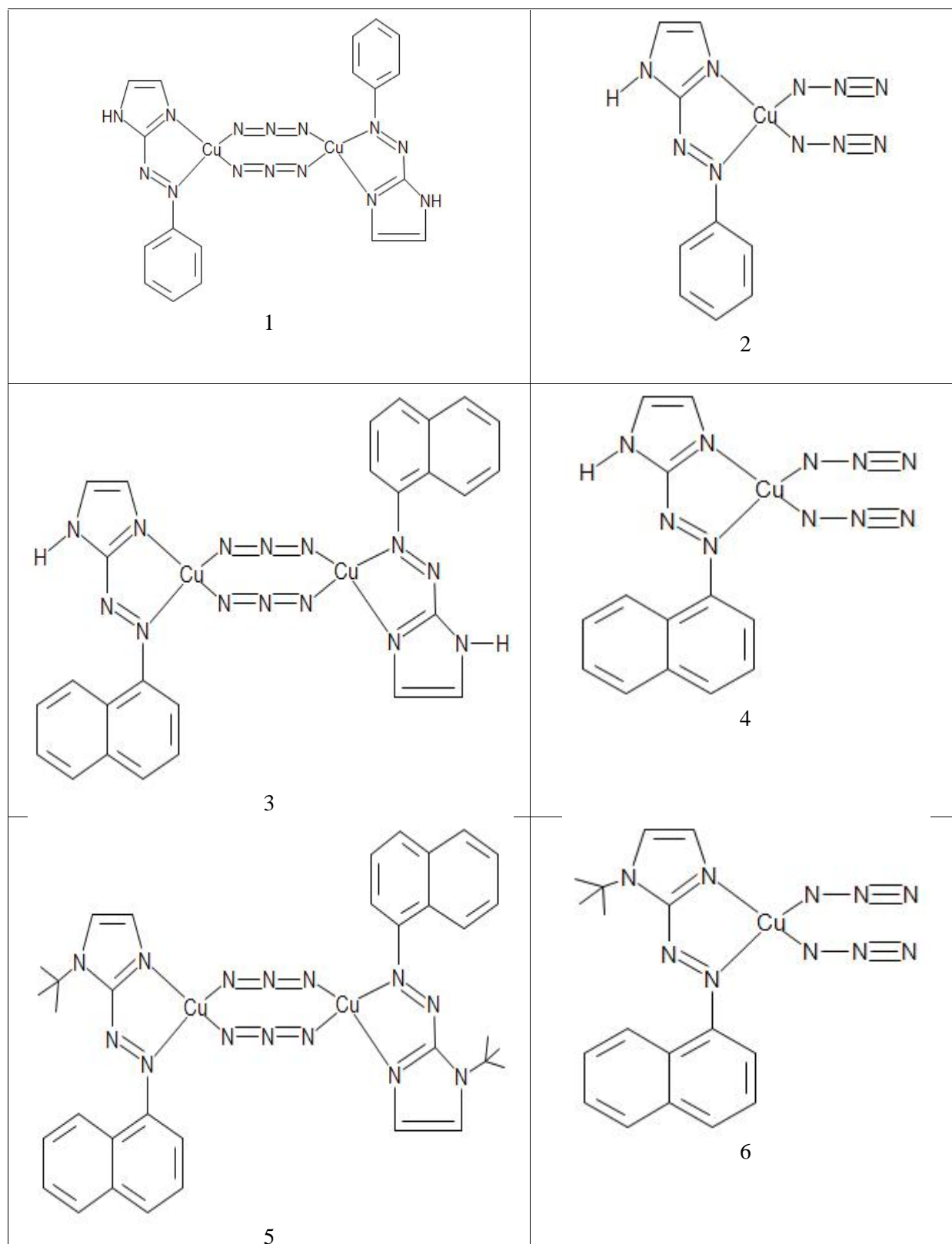
Synthesis of the Compound 13: NaPY(0.0593g =0.00026mole) + CuCl_2 (0.0443g=1eqv) + NaN_3 (0.0169g=1eqv), Solvent use –Acetone/sharp colour change was observed. .0593g i.e 0.00026 mole NaPY was dissolved in acetone solvent .0443g of CuCl_2 i.e 1 equivalent was added into this solution. Now 0.0169g i.e 1 eqv of NaN_3 was added into the mixture and the colour change was observed. The whole mixture was stirred for 12 hours. After the completion of the reaction it was filtered & filtrates was collected for crystal tube setting and for another charecterisation analysis of the compound.

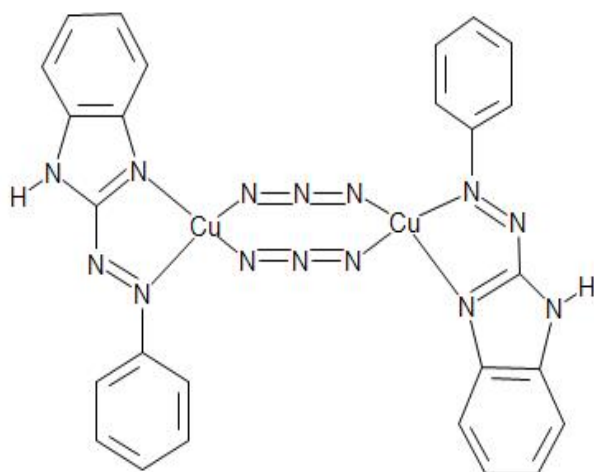
Characterisation of the Compound 13: CHN calculation of the above compound $[\text{C}_{32}\text{H}_{24}\text{N}_{10}\text{Cu}_2]$, gives Calc(found): C, 56.88 (56.9), H, 35.80 (35.8), N, 20.73(20.7); IR Spectroscopic data, $\nu(\text{N}=\text{N})$ 1370 $\nu(\text{C}=\text{N})$ 1590, ESI/MS Spectroscopic data, 675.6 $[\text{M}^+]$, Proton n.m.r.Spectroscopic data, ^1H , ppm, 8.07(d, $J = 8\text{Hz}$, H(7,11)), 8.01(d, $J=6.5\text{Hz}$, H(8,10)), 7.09(m, 9-H), 7.26(d, $J=6\text{Hz}$, H(4)), 7.34(d, $J=5\text{Hz}$, H(5)), 1.5(s, N-Me); UV-Vis Spectroscopic data, (nm), 244(10500), 280(8160), 282(8200), 295(600),(sh); Electrochemistry or Cyclic Voltammetric data ($E_{1/2}$ (V) (E_p (mV) [Solvent MeCN, Supporting Electrolyte, Bu_4NClO_4 (0.1 M), scan rate 50 mVs^{-1} , Pt disk working electrode, Pt wire auxiliary electrode, reference electrode SCE at 298 K] ligand reduction -0.66 (100).

Fig. 1: Reaction scheme and all the mononuclear and binuclear complexes of copper from complex 1 to complex 14, $[\text{Cu}(\text{N}_3)_2(\text{NaaiR}')_2]$ and $[\text{Cu}_2(--\text{N}_3)_2(\text{NaaiR}')_2]$, $[\text{NaaiR}' = \text{naphthyl-azo imidazole/benzimidazole/pyridine} = \text{C}_{10}\text{H}_4\text{-N}=\text{N-} / \text{C}_3\text{H}_2\text{-NN-1-R}'$, (R imidazole) / $\text{C}_7\text{H}_4\text{-NN-1-H}$ (Benzimidazole), / $\text{C}_3\text{H}_4\text{-N-}$ (Pyridine), abbreviated as N,N'-chelator, where N(imidazole) and N(azo) represent N and N', respectively; R' = H(a), Me (b), $\text{N}_3 = \text{monodentate azide linkage}$, $--\text{N}_3 = \text{azide bridged binuclear complex}$].

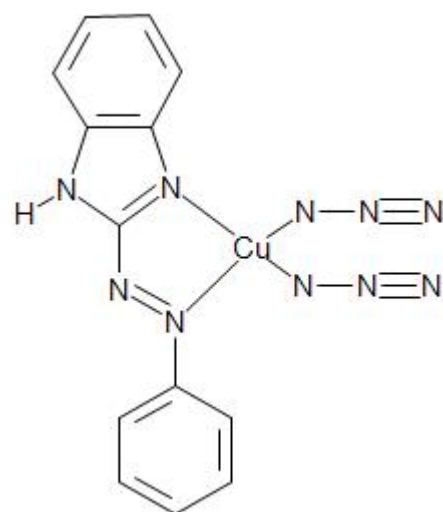
Synthesis of the compound 14: NaPY (0.0668g =0.00029mole) + CuCl_2 (0.0494g=1eqv) + NaN_3 (0.0377g=2eqv), Solvent use –Acetone/sharp colour change was observed. .0668g i.e 0.00029 mole NaPY was dissolved in acetone solvent 0.0494 of CuCl_2 i.e 1 equivalent was added into this solution. Now 0.0377g i.e 2 eqv of NaN_3 was added into the mixture and the colour change was observed. The whole mixture was stirred for 12 hours.after the completion of the reaction it was filtered & filtrate was collected for crystal tube setting and for another charecterisation analysis of the compound.

Characterisation of the Compound 14: CHN calculation of the above compound $[\text{C}_{14}\text{H}_{12}\text{N}_8\text{Cu}_1]$, gives Calc(found): C, 50.59(50.6), H, 3.18 (3.18), N, 29.49(29.5); IR Spectroscopic data, $\nu(\text{N}=\text{N})$ 1370 $\nu(\text{C}=\text{N})$ 1590, ESI/MS Spectroscopic data, 379.8 $[\text{M}^+]$, Proton n.m.r.Spectroscopic data, ^1H , ppm, 8.07(d, $J = 8\text{Hz}$, H(7,11)), 8.01(d, $J=6.5\text{Hz}$, H(8,10)), 7.09(m, 9-H), 7.26(d, $J=6\text{Hz}$, H(4)), 7.34(d, $J=5\text{Hz}$, H(5)), 1.5(s, N-Me); UV-Vis Spectroscopic data, (nm), 244(10500), 280(8160), 282(8200), 295(600),(sh); Electrochemistry or Cyclic Voltammetric data ($E_{1/2}$ (V) (E_p (mV) [Solvent MeCN, Supporting Electrolyte, Bu_4NClO_4 (0.1 M), scan rate 50 mVs^{-1} , Pt disk working electrode, Pt wire auxiliary electrode, reference electrode SCE at 298 K] ligand reduction -0.76 (70).

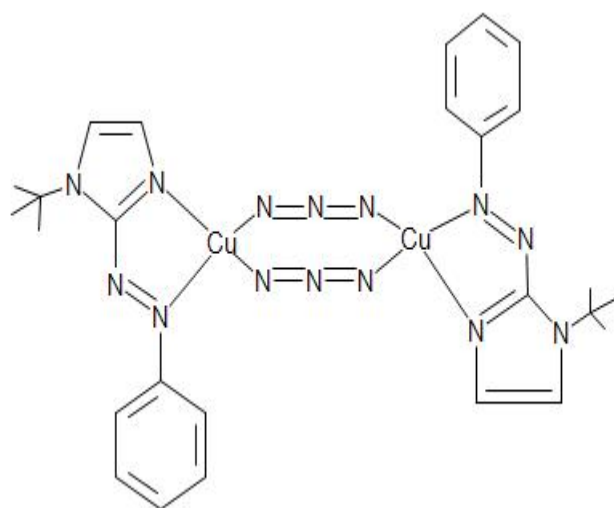




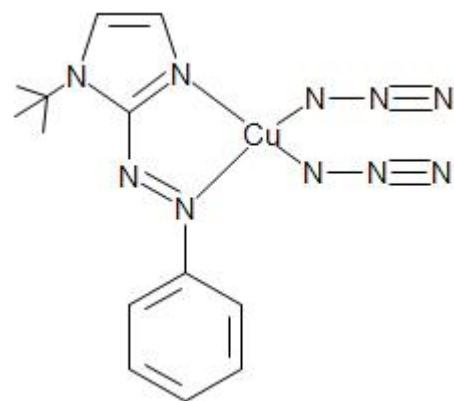
7



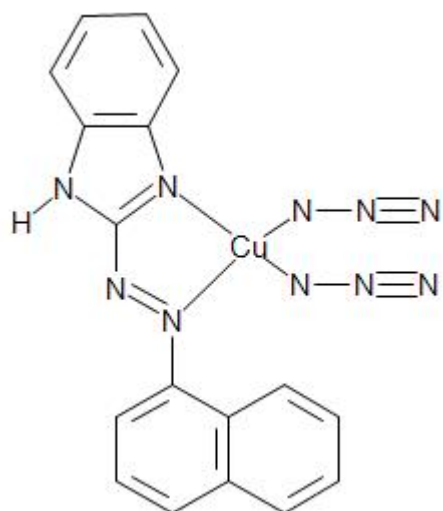
8



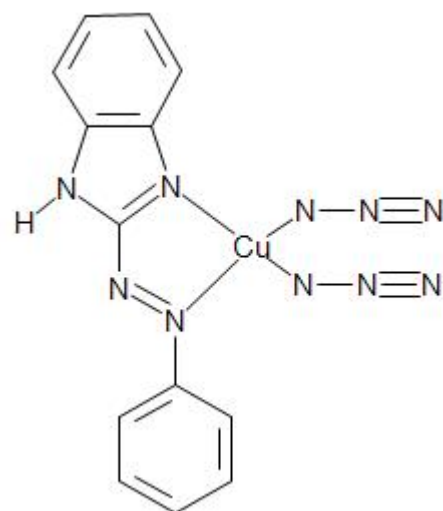
9



10



11



12

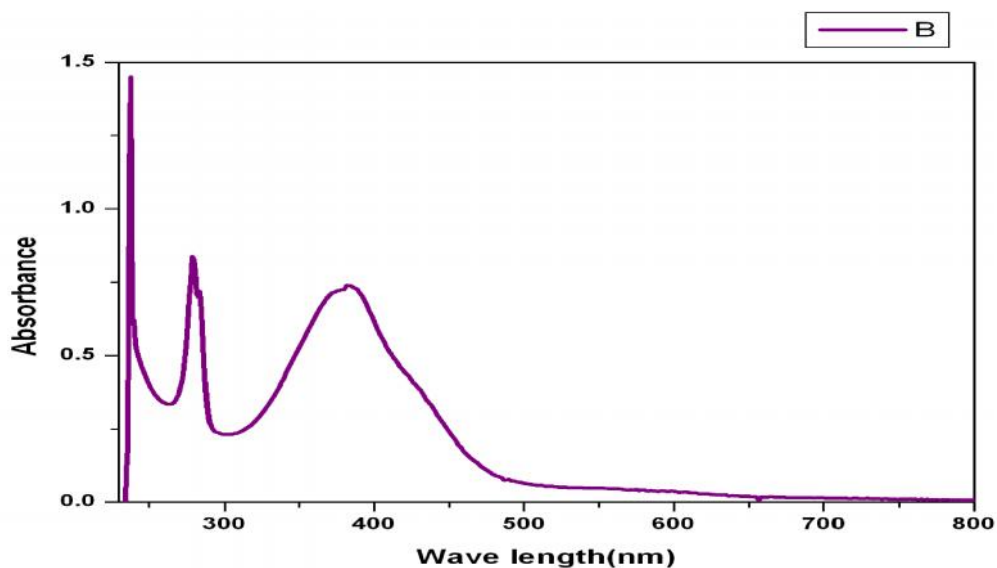
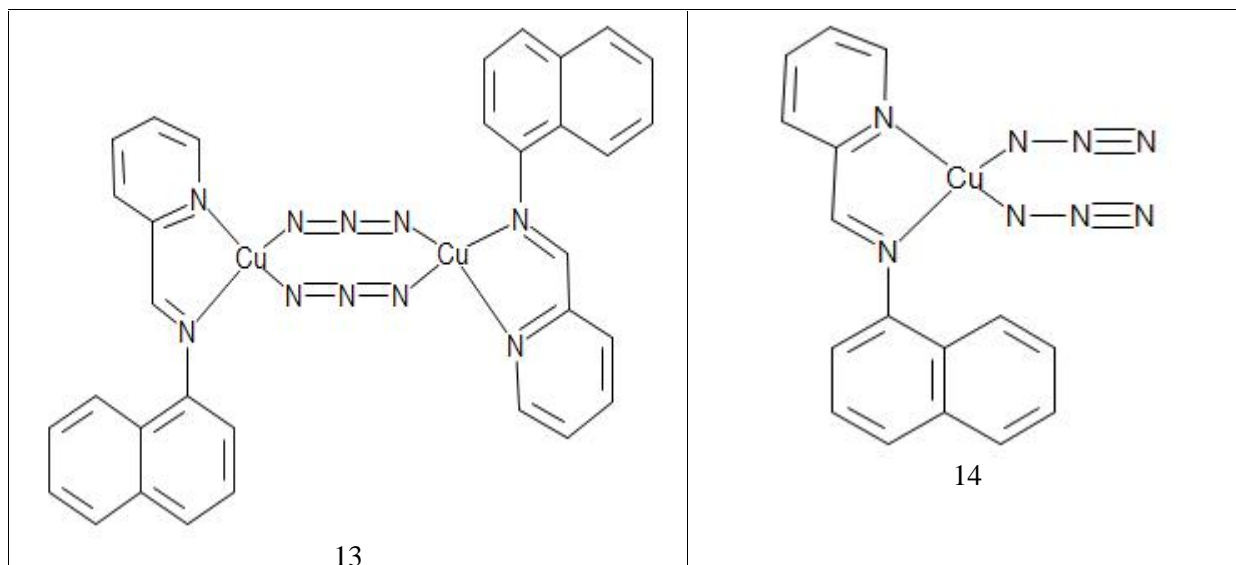


Figure 2: UV-Vis Spectroscopic data, (nm), of complex $[\text{Cu}_2(\text{--N}_3)_2(\text{NaaiR}')_2]$, 13.

RESULTS AND DISCUSSION

Synthesis and Formulation

Reaction of copper perchlorate hexahydrate $[\text{Cu}(\text{H}_2\text{O})_6](\text{ClO}_4)_2$ with NaaiR' in CH_2Cl_2 or acetone medium following ligand addition leads to $[\text{Cu}(\text{N}_3)_2(\text{NaaiR}')_2]$ and $[\text{Cu}_2(\text{--N}_3)_2(\text{NaaiR}')_2]$, [$\text{NaaiR}' = \text{naphthyl-azo imidazole / benzimidazole / pyridine} = \text{C}_{10}\text{H}_4\text{-N=N-} / \text{C}_7\text{H}_4\text{-NN-1-R}'$, (R imidazole) / $\text{C}_7\text{H}_4\text{-NN-1-H}$ (Benzimidazole), / $\text{C}_3\text{H}_4\text{-N-}$ (Pyridine), abbreviated as $\text{N,N}'$ -chelator, where N(imidazole) and N(azo) represent N and N' , respectively; $\text{R}' = \text{H}(a)$, $\text{Me}(b)$, $\text{N}_3 = \text{monodentate azide linkage}$, $\text{--N}_3 = \text{azide bridged binuclear complex}$]. were prepared by removing H_2O , with NaaiR under stirring at 343-353 K in MeOH solution in poor yield (35-40%). The composition of the complexes is supported by microanalytical results. The red orange complexes are soluble in common organic solvents viz. acetone, acetonitrile, chloroform, dichloromethane but not soluble in H_2O , methanol, ethanol. The voltammogram also shows a small anodic peak at 0.2 V, possibly due to the Cu (I)/Cu (0) couple.

Spectral Studies

I.r. spectra of the complexes, show a 1:1 correspondence to the spectra of the chloro analogue, except the appearance of intense stretching at 1365-1370 and 1570-1580 cm^{-1} with concomitant loss of $\nu(\text{Cu-Cl})$ at 320-340 cm^{-1} . They are assigned to $\nu(\text{N=N})$ and $\nu(\text{C=N})$ appear at 1365-1380 and 1570-1600 cm^{-1} , respectively.

The ESI mass spectrum of a 1:1, MeCN: H_2O solution in the positive ion mode is structurally enlightening, since it displays a series of characteristic singly. Population of gas phase ions generated by ESI often closely reflects that in solution.

The electronic spectra of the complexes exhibit multiple high intense transitions in 450–250 nm along with a weak transition at 700–710 nm. In free ligand, the intra-ligand charge transfer, $n\text{-p}^*$ and $p\text{-p}^*$, appear at 370–380 and 250–260 nm, respectively. Low energy weak transition at 700–710 nm (Fig. 2) may be referred to $d\text{-}d$ band. Copper(II)–azo-heterocycle and azide bridged heterocycles show the MLCT transition involving $d(\text{Cu}) \rightarrow p^*$ (Naphthylazoheterocycle) at longer wavelength (>400 nm). It is due to efficient p -acidity of the ligands. On comparing with copper(II) complexes of 1-alkyl-2-(ary-lazo)imidazoles, pyridyl-thioazophenolates and other pyridylthioether ligands the transitions at 430 nm is assigned to MLCT [$d(\text{Cu}) \rightarrow p^*$ (naphthyl-azo-imidazole)] and, the band at 370 nm may be a mixture of $S(\text{thioether})\text{-Cu(II)}$ and ligand centered $p\text{-}p^*$ transitions (Fig. 2).

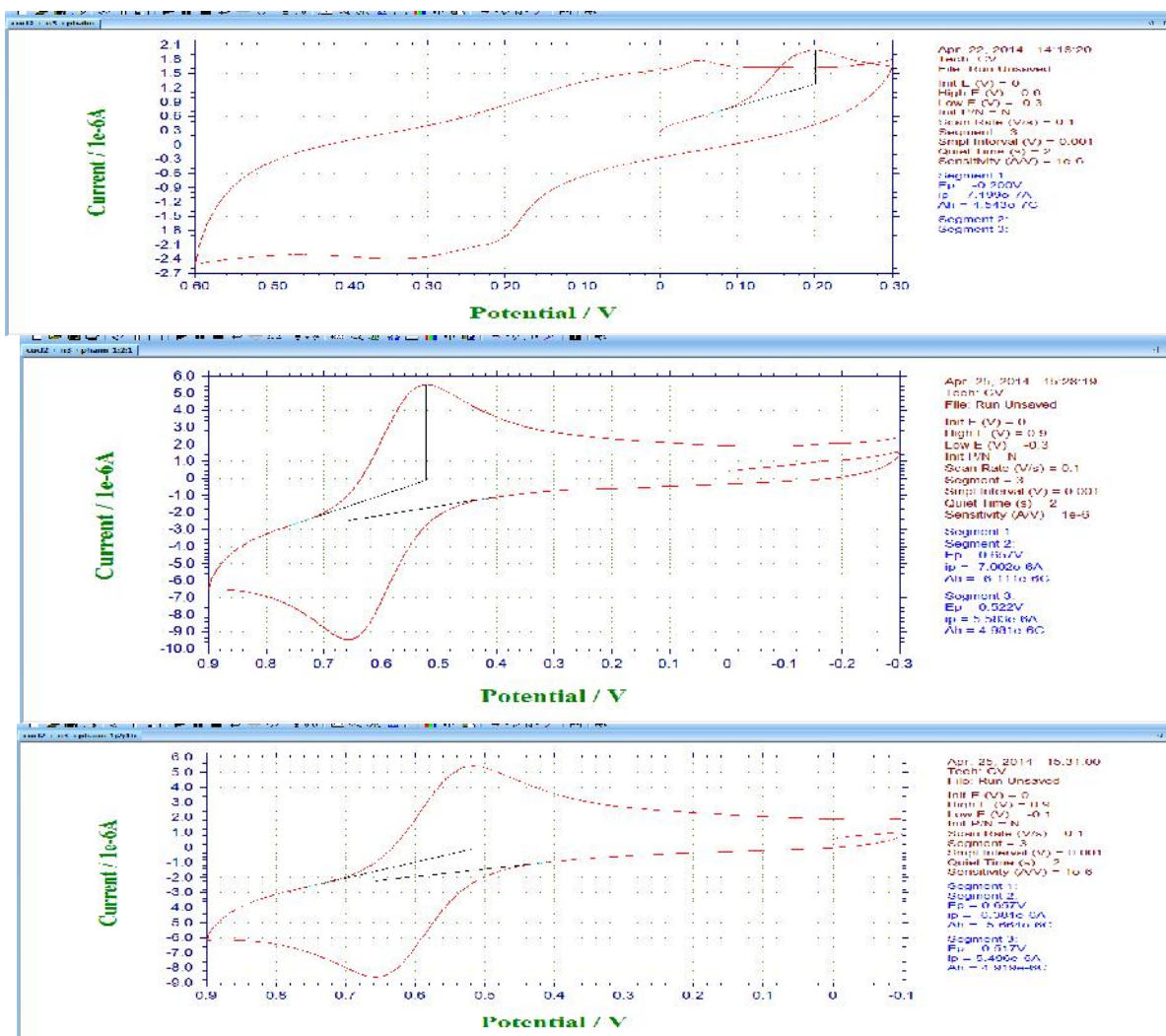
The ^1H n.m.r. spectra, measured in CD_2Cl_2 , of $[\text{Cu}(\text{N}_3)_2(\text{NaaiR}')_2]$ and $[\text{Cu}_2(\text{-N}_3)_2(\text{NaaiR}')_2]$, [$\text{NaaiR}' = \text{naphthyl-azo imidazole /benzimidazole /pyridine} = \text{C}_{10}\text{H}_4\text{-N=N-} / \text{C}_3\text{H}_2\text{-NN-1-R}'$, (R imidazole) / $\text{C}_7\text{H}_4\text{-NN-1-H}$ (Benzimidazole), / $\text{C}_3\text{H}_4\text{-N-}$ (Pyridine), abbreviated as $\text{N,N}'\text{-chelator}$, where $\text{N}(\text{imidazole})$ and $\text{N}(\text{azo})$ represent N and N' , respectively; $\text{R}' = \text{H}(a)$, $\text{Me}(b)$, $\text{N}_3 = \text{monodentate azide linkage}$, $\text{-N}_3 = \text{azide bridged binuclear complexes}$] were unambiguously assigned on comparing with $[\text{Cu}(\text{H}_2\text{O})]$ and the free ligand (NaaiR'). Imidazole 4- and 5-H appear as doublet at the lower frequency side of the spectra (7.0-7.2 ppm for 4-H; 6.9-7.1 ppm for 5-H). The aryl protons (7-H—11-H) of (7-9) are downfield shifted by 0.1-0.7 ppm as compared to those of the parent derivatives. They are affected by substitution; 8- and 10-H are severely perturbed due to changes in the electronic properties of the substituents in the C(9)-position. The aryl protons 7-(7'-) and 11-(11'-)H resonate asymmetrically indicative of a magnetically anisotropic environment even in the solution phase.

The ^{13}C NMR spectrum, measured in CD_2Cl_2 , provides direct information about the carbon skeleton of the molecule $[\text{Cu}(\text{N}_3)_2(\text{NaaiR}')_2]$ and $[\text{Cu}_2(\text{-N}_3)_2(\text{NaaiR}')_2]$, [$\text{NaaiR}' = \text{naphthyl-azo imidazole /benzimidazole /pyridine} = \text{C}_{10}\text{H}_4\text{-N=N-} / \text{C}_3\text{H}_2\text{-NN-1-R}'$, (R imidazole) / $\text{C}_7\text{H}_4\text{-NN-1-H}$ (Benzimidazole), / $\text{C}_3\text{H}_4\text{-N-}$ (Pyridine), abbreviated as $\text{N,N}'\text{-chelator}$, where $\text{N}(\text{imidazole})$ and $\text{N}(\text{azo})$ represent N and N' , respectively; $\text{R}' = \text{H}(a)$, $\text{Me}(b)$, $\text{N}_3 = \text{monodentate azide linkage}$, $\text{-N}_3 = \text{azide bridged binuclear complex}$]. The non-protonated carbon atoms at C(2) and C(6) of the naphthylazoimidazole moiety is shifted farthest downfield in the spectrum. The carbon atom adjacent to the benzimidazole, naphthyl, molecule in the complex resonance at a lower field resulting of the conjugative effect of the phenyl ring with more electronegative π -conjugate system. The methyl carbon atom of the imidazole ring resonate at 30 ppm, reasonably compare to the other carbon atoms resonance.

Electrochemistry

Fig. 3, Fig. 4 and Fig. 5 shows representative cyclic voltammogram of the complexes and data are collected in Experimental Section. Copper(I) complexes, $[\text{Cu}(\text{N}_3)_2(\text{NaaiR}')_2]$ and $[\text{Cu}_2(\text{-N}_3)_2(\text{NaaiR}')_2]$, [$\text{NaaiR}' = \text{naphthyl-azo imidazole /benzimidazole /pyridine} = \text{C}_{10}\text{H}_4\text{-N=N-} / \text{C}_3\text{H}_2\text{-NN-1-R}'$, (R imidazole) / $\text{C}_7\text{H}_4\text{-NN-1-H}$ (Benzimidazole), / $\text{C}_3\text{H}_4\text{-N-}$ (Pyridine), abbreviated as $\text{N,N}'\text{-chelator}$, where $\text{N}(\text{imidazole})$ and $\text{N}(\text{azo})$ represent N and N' , respectively; $\text{R}' = \text{H}(a)$, $\text{Me}(b)$, $\text{N}_3 = \text{monodentate azide linkage}$, $\text{-N}_3 = \text{azide bridged binuclear complex}$], show a quasireversible oxidative response at 0.4 V which may be referred to Cu(II)/Cu(I) . An irreversible response is observed at 1.0 V that may be assigned to

the oxidation of water present in solvent. On scanning to ve direction up to 1.8 V we observe an irreversible response E_{pc} at 0.4 V and a quasireversible response at 1.1 to 1.3 V. They may be assigned to reduction of azo group $[(-N@N-)/(-N@N-)]$ of the chelated ligands. The voltammogram also shows a small anodic peak at 0.2 V, possibly due to the Cu(I)/Cu(0) couple. The reduced Cu(0) is absorbed on the electrode surface as evidenced from the narrow width of the anodic response with a large peak current. In case of [Cu of the couple at 0.4 V is largely dependent on scan rate and increases from 100 mV at remains almost constant and also the values when the voltammogram is scanned at slow scan rates (10–50 mV s⁻¹). This observation suggests low heterogeneous electron-transfer rate constant which has been influenced by the applied potential. In general, the electrochemical reduction of copper (II) complexes is associated with change in coordination geometry. Solution structure of copper (II) complex shows square pyramidal or trigonal bipyramidal which upon reduction rearranges fast to tetrahedral geometry via bond rupture and bond formation. Two couples at ca.0.5 and 1.2 V are assigned to azo reduction. The quasireversibility of the couples are noted by peak-to-peak separation.



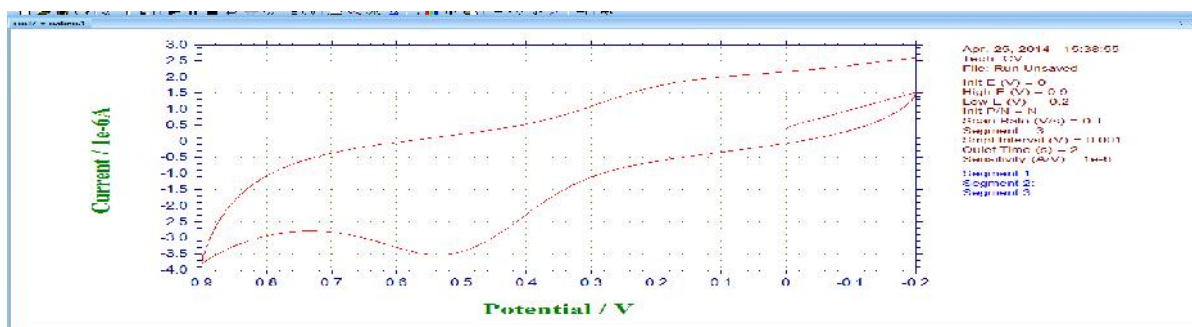
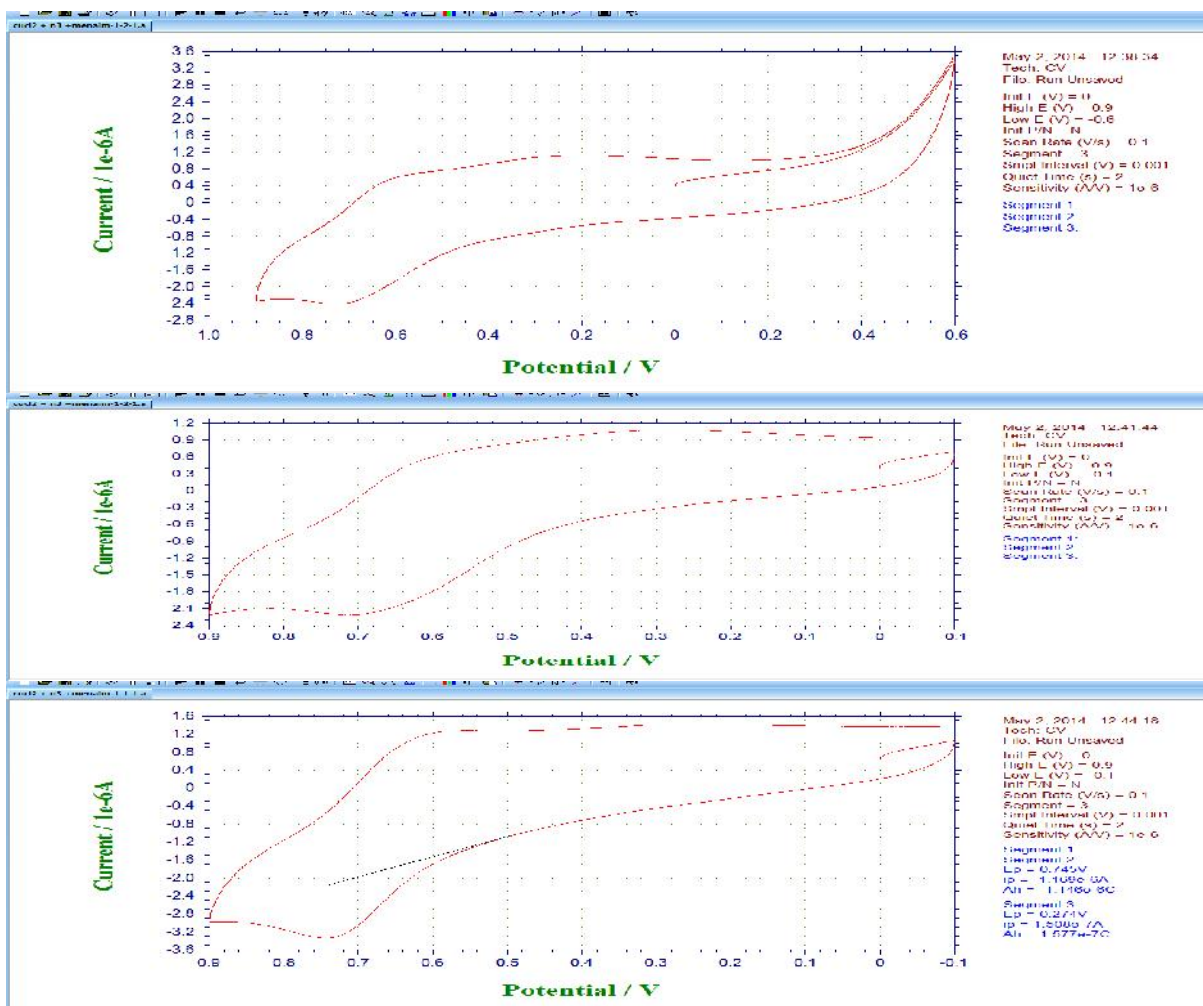


Figure 3: Electrochemistry or Cyclic Voltammetric data ($E_{1/2}$ (V) (E_p (mV) [Solvent MeCN, Supporting Electrolyte, Bu_4NClO_4 (0.1 M), scan rate 50 mVs^{-1} , Pt disk working electrode, Pt wire auxiliary electrode, reference electrode SCE at 298 K] of complex 1 (above two) and 2 (below two).



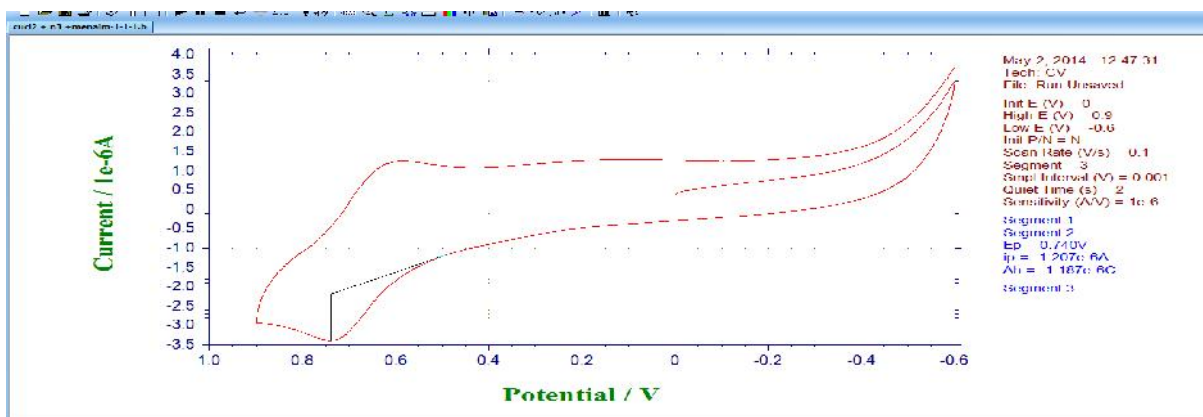


Figure 4: Electrochemistry or Cyclic Voltammetric data ($E_{1/2}$ (V) (E_p (mV) [Solvent MeCN, Supporting Electrolyte, Bu_4NClO_4 (0.1 M), scan rate 50 mVs^{-1} , Pt disk working electrode, Pt wire auxiliary electrode, reference electrode SCE at 298 K] of complex 13 and 14.

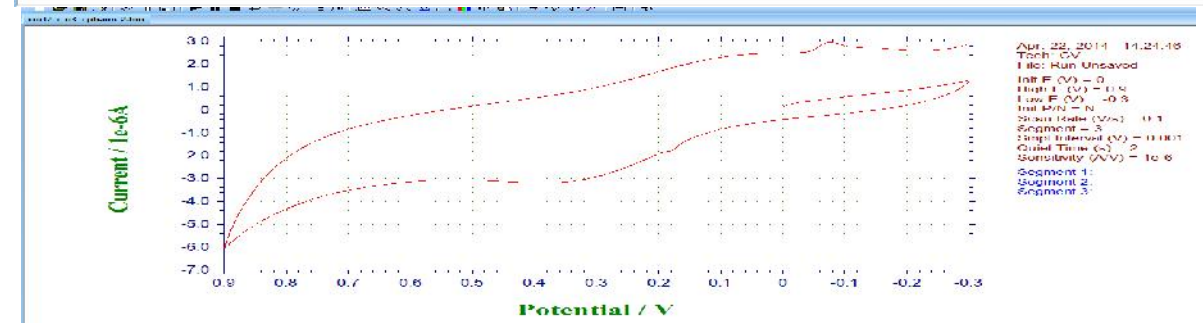
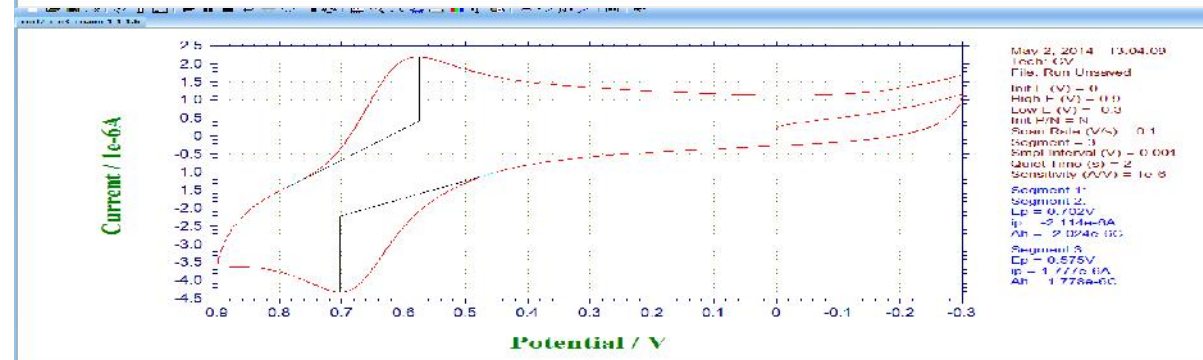
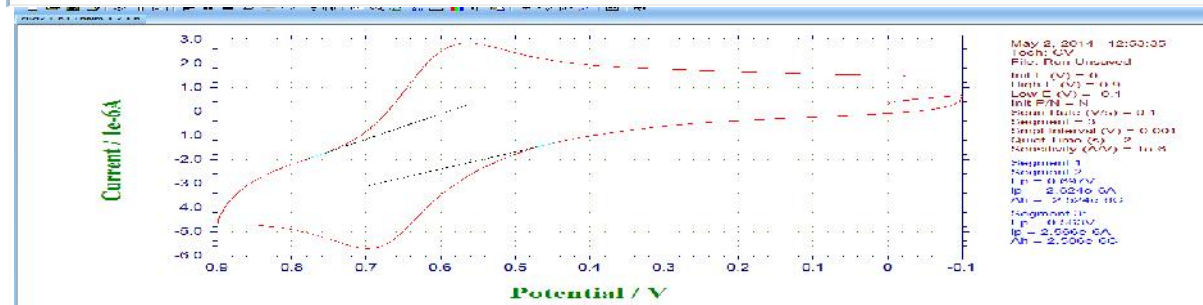
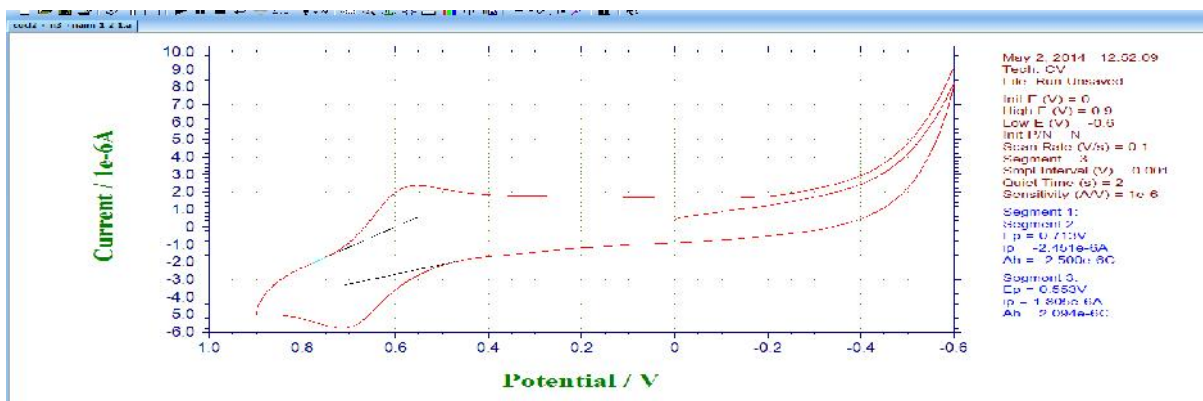


Figure 5: Electrochemistry or Cyclic Voltammetric data ($E_{1/2}$ (V) (E_p (mV) [Solvent MeCN, Supporting Electrolyte, Bu_4NClO_4 (0.1 M), scan rate 50 mVs^{-1} , Pt disk working electrode, Pt wire auxiliary electrode, reference electrode SCE at 298 K] of complex 5 and 6.

CONCLUSION

This work describes the isolation of a novel series of copper(II) azo-imine mononuclear and binuclear azide bridged complexes, $[Cu(N_3)_2(NaaiR')_2]$ and $[Cu_2(--N_3)_2(NaaiR')_2]$, $[NaaiR' = \text{naphthyl-azo imidazole /benzimidazole /pyridine} = C_{10}H_4-N=N- / C_3H_2-NN-1-R', (R \text{ imidazole}) / C_7H_4-NN-1-H \text{ (Benzimidazole)}, / C_3H_4-N-(\text{Pyridine})$, abbreviated as N,N' -chelator, where $N(\text{imidazole})$ and $N(\text{azo})$ represent N and N' , respectively; $R' = H(a)$, $Me (b)$, $N_3 = \text{monodentate azide linkage, } --N_3 = \text{azide bridged binuclear complex}$], and their spectral and elemental characterisation. The complexes were well characterised by NMR, IR, UV VIS, CV, Mass spectroscopy. The voltammogram also shows a small anodic peak at 0.2 V, possibly due to the $Cu(I)/Cu(0)$ couple.

ACKNOWLEDGEMENTS

Department of Science and Technology (DST) are thanked for financial support (FAST TRACK Grand No. SERB/F/4888/2012-13 Dated 30.11.2012, Project Title: Gold (I) & Gold(II) Arylazoimidazole (N, N Donor) & Oxo Complexes : Synthesis, Structure, Spectral Study, Electrochemistry And Chemical Reactivity.

REFERENCE

- Byabartta Prithwiraj, Sau Somnath. 2014. Copper (II) Azo Complexes: Copper (II)-Bis Naphthylazo Imidazole/ Benzimidazole/ Pyridine Complexes: Synthesis and Spectroscopic Study and Electrochemistry. *The Journal of Applied Sciences*. Vol 1, No 2.
- Byabartta Prithwiraj. 2014a. Synthesis, Spectroscopy and Electrochemistry of nitroso terpyridine-{1-(alkyl)-2-(arylazo) imidazole} ruthenium (II) Complexes. *The Journal of Applied Sciences*. Vol 1, No 1.
- Byabartta Prithwiraj. 2014b Gold (III)-2,2'-Bipyridine(bpy)-Arylazoimidazole (RaaiR') Complexes: Synthesis and Spectral Characterisation, *The Journal of Applied Sciences*. Vol 1, No 2.
- Byabartta, P., Santra P. K., Misra T. K., Sinha C. and Kennard C. H. L. 2001. Synthesis, spectral characterization, redox studies of isomeric dichlorobis-[1-alkyl-2-(naphthyl-(α/β)-azo)imidazole]ruthenium(II). Single crystal X-ray structure of blue-green *dichloro-bis-[1ethyl2-(naphthyl-r-azo)imidazole]ruthenium(II)*, *Polyhedron*. 20:905.
- Byabartta, P., Jasimuddin Sk., Mostafa G., Lu T. – H. and Sinha C., 2003. The synthesis, spectral studies and electrochemistry of 1,10-(phenanthroline)-bis-{1-alkyl-2-(arylazo)imidazole}ruthenium(II) perchlorate. Single crystal X-ray structure of $[Ru(\text{phen})(\text{HaaiMe})_2](\text{ClO}_4)_2$ [$\text{phen} = 1,10\text{-phenanthroline}$, $\text{HaaiMe} = 1\text{-methyl-2-(phenylazo)imidazole}$] *Polyhedron*, 22.
- Venkanna Avudoddi, Swapna Kokkerala and Rao Pallapothula Venkateswar. 2014. Recyclable nano copper oxide catalyzed synthesis of quinoline-2,3-dicarboxylates under ligand free conditions, *RSC Adv.*, 2014,4, 15154-15160, DOI: 10.1039/C3RA47212D.
- Kim Ki-Joong, Oleksak Richard Paul, Pan Changqing, Knapp Michael Wayne, Kreider Peter, 2014. Herman Gregory and Chang Chih-hung, Continuous Synthesis of Colloidal Chalcopyrite Copper Indium Diselenide Nanocrystal Inks , *RSC Adv.*, 2014; DOI: 10.1039/C4RA01582G,
- Huang Xin, Wang Jichao, Ni Zhangqin, Wang Sichang and Pan Yuanjiang, 2014. Copper-mediated S–N formation *via* an oxygen-activated radical process: a new synthesis method for sulfonamides, *Chem. Commun.*, DOI: 10.1039/C4CC01353K.
- Loganathan Rangasamy, Ramakrishnan Sethu, Suresh Eringathodi, Palaniandavar Mallayan, Riyasdeen Anvarbatcha and Abdulkadhar Mohamad, 2014. Mixed ligand μ -phenoxo-bridged dinuclear copper(II) complexes with diimine co-ligands: efficient chemical nuclease and protease activities and cytotoxicity, *Dalton Trans.*, 2014,43, 6177-6194 .DOI: 10.1039/C3DT52518J.
- Kang Kai, Xu Chunfa and Shen Qilong. 2014. Copper-catalyzed trifluoromethylthiolation of aryl and vinyl boronic acids with a shelf-stable electrophilic trifluoromethylthiolating reagent, *Org. Chem. Front.*, 2014,1, 294-297, DOI: 10.1039/C3QO00068K.

- Sapuppo Giulia, Wang Qian, Swinnen Dominique and Zhu Jieping, 2014. Copper-catalyzed three-component synthesis of 5-acetamidoimidazoles from carbodiimides, acyl chlorides and isocyanides, *Org. Chem. Front.*, 2014,1, 240-246 .DOI: 10.1039/C4QO00034J.
- Chen Yan-Fu, Wu Yi-Sheng, Jhan Yu-Huei and Jen-Chieh Hsieh, 2014. An efficient synthesis of (NH)-phenanthridinones *via* ligand-free copper-catalyzed annulation, *Org. Chem. Front.*, 2014,1, 253-257 , DOI: 10.1039/C3QO00082F.
- Espinosa Daniel Mendoza-, Negrón-Silva Guillermo Enrique, Ángeles-Beltrán Deyanira, Alejandro Álvarez-Hernández, Oscar R. Suárez-Castillo and Rosa Santillán, 2014. Copper(II) complexes supported by click generated mixed *NN*, *NO*, and *NS* 1,2,3-triazole based ligands and their catalytic activity in azide-alkyne cycloaddition, *Dalton Trans.*, 2014; DOI: 10.1039/C4DT00323C.
- Takemura Noriaki, Kuninobu Yoichiro and Kanai Motomu, 2012. Copper-catalyzed benzylic C(sp³)-H alkoxylation of heterocyclic compounds, *Org. Biomol. Chem.*, 12, 2528-2532 .DOI: 10.1039/C4OB00215F.
- Lauria Antonino, Bonsignore Riccardo, Terenzi Alessio, Spinello Angelo, Francesco Giannici, Longo Alessandro, Maria Almerico Anna and Barone Giampaolo, 2014. Nickel(II), copper(II) and zinc(II) metallo-intercalators: structural details of the DNA-binding by a combined experimental and computational investigation, *Dalton Trans.* 2014,43, 6108-6119 DOI: 10.1039/C3DT53066C.
- Yang Fei, Wei Jingjing, Wei Liu, Jinxin Guo and Yanzhao Yang, 2014. Copper doped ceria nanospheres: surface defects promoted catalytic activity and a versatile approach, *J. Mater. Chem. A*, 2014,2, 5662-5667, DOI: 10.1039/C3TA15253G.
- Harutyunyan Syuzanna R, Oost Rik, Jiawei Rong and Adriaan J Minnaard , 2014. Synthesis of new derivatives of copper complexes of Josiphos family ligands for applications in asymmetric catalysis, *Catal. Sci. Technol.*, 2014; DOI: 10.1039/C4CY00180J.
- Kumari Harshita, Mossine Andrew V., Schuster Nathaniel J., Charles L. Barnes, Carol A. Deakne and Jerry L. Atwood, 2014. Packing arrangements of copper-seamed C-alkylpyrogallol[4]arene nanocapsules with varying chain lengths , *CrystEngComm*, 2014; DOI: 10.1039/C3CE42412J.
- Venkatakrisnan Showmya, Veerappan Ganapathy, Elamparuthi Elangovan and Anbazhagan Veerappan, 2014. Aerobic synthesis of biocompatible copper nanoparticles: promising antibacterial agent and catalyst for nitroaromatic reduction and C-N cross coupling reaction, *RSC Adv.*, 2014,4, 15003-15006, DOI: 10.1039/C4RA01126K.
- Leung King Pong, Chen Dongshi and Chan King Ming, 2014. Understanding copper sensitivity in zebrafish (*Danio rerio*) through the intracellular localization of copper transporters in a hepatocyte cell-line ZFL and the tissue expression profiles of copper transporters, *Metallomics*, 2014; DOI: 10.1039/C3MT00366C.
- Kim Sang-Min, Kim Jae-Hyun, Kim Kwang-Seop, Yun Hwangbo, Jong-Hyuk Yoon, Eun-Kyu Lee, Jaechul Ryu, Hak-Joo Lee, Seungmin Cho and Seung-Mo Lee, 2014. Synthesis of CVD-graphene on rapidly heated copper foils, *Nanoscale*, 2014; DOI: 10.1039/C3NR06434D,
- Cadot Stéphane, Rameau Nelly, Mangematin Stéphane, Pinel Catherine and Laurent DJAKOVITCH, 2014. Preparation of functional styrenes from biosourced carboxylic acids by copper catalyzed decarboxylation in PEG, *Green Chem.*, 2014; DOI: 10.1039/C4GC00256C.
- Papaefstathiou Giannis S., Subrahmanyam Kota S., Armatas Gerasimos S., Malliakas Christos D., Kanatzidis Mercouri G. and Manos Manolis J., 2014. A unique microporous copper trimesate selenite with high selectivity for CO₂, *CrystEngComm*, 2014; DOI: 10.1039/C4CE00091A.,
- Vidhyadharan Baiju, Misnon Izan Izwan, Aziz Radhiyah Abd, Padmasree K. P., Yusoff Mashitah M. and Rajan Jose ,2014. Superior supercapacitive performance in electrospun copper oxide nanowire electrodes, *J. Mater. Chem. A*, 2014; DOI: 10.1039/C3TA15304E.
- Zhao Lianchao, Yan Hongtao, Caixia Yang and Jiping Pan, 2014. Fabrication and application of a copper(II)-selective extraction disc prepared from chlorinated polyvinyl chloride and ethylenediamine-functionalized cellulose, *Anal. Methods*, 2014; DOI: 10.1039/C3AY41890A.
- Hassan Iman, Parkin Ivan P, Nair Sean and Carmalt Claire J, 2014. Antimicrobial Activity of Copper and Copper(I) Oxide Thin Films Deposited via Aerosol-Assisted CVD, *J. Mater. Chem. B*, 2014; DOI: 10.1039/C4TB00196F.
- Sebio Rosario Musacco, Ferrarotti Nidia, Christian Saporito-Magriñá, Jimena Semprine, Julián Fuda, Horacio Torti, Alberto Boveris and Marisa. 2014. Rat brain oxidative damage in iron and copper overloads. *Metallomics*. DOI: 10.1039/C3MT00378G.
- Xu jiao shuang, Chen Funan, Deng Mao and Yanyan Sui. 2014. Luminol chemiluminescence enhanced by copper nanoclusters and its analytical application *RSC Adv*. DOI: 10.1039/C4RA00516C.

- Tian Hao, Zhang Xiao Li, Scott Jason, Charlene Ng and Rose Amal. 2014. TiO₂-supported copper nanoparticles prepared *via* ion exchange for photocatalytic hydrogen production. *J. Mater. Chem.* DOI: 10.1039/C3TA15254E.
- Nasr-Esfahani Mahboobeh, Mohammadpoor-Baltork Iraj, Khosropour Ahmad Reza, Majid Moghadam, Valiollah Mirkhani, Shahram Tangestaninejad, Vladislav Agabekov and Hadi Amiri Rudbari. 2014. Copper immobilized on nano-silica triazine dendrimer (Cu(II)-TD@nSiO₂) catalyzed synthesis of symmetrical and unsymmetrical 1,3-diyne under aerobic conditions at ambient temperature. *RSC Adv.* 4:14291-14296. DOI:10.1039/C3RA47184E.
- Chen Zuofeng, Ye Shengrong, Adria R. Wilson, Yoon-Cheol Ha and Benjamin J. Wiley, Optically transparent hydrogen evolution catalysts made from networks of copper-platinum core-shell nanowires. *Energy Environ. Sci.* 7:1461-1467. DOI: 10.1039/C4EE00211C.
- Qu Zhi-Kun, Yu Kai, Zhao Zhi-Feng, Su Zhan-hua, Sha Jing-Quan, Chun-Mei Wang and Bai-Bin Zhou. 2014. An organic-inorganic hybrid semiconductor material based on Lindqvist polyoxomolybdate and a tetra-nuclear copper complex containing two different ligands. *Dalton Trans.*, 2014; DOI: 10.1039/C3DT53345J.
- Xi Pinxian, Xu Zhihong, Gao Daqiang, Chen Fengjuan, Desheng Xue, Chun-Lan Tao and Zhong-Ning Chen. 2014. Solvothermal synthesis of magnetic copper nitride nanocubes with highly electrocatalytic reduction properties. *RSC Adv.* 4:14206-14209. DOI: 10.1039/C4RA01307G.
- Lu Hang, Yu Li, Yang Bo, Jianing Si and Jianzhong Du. 2014. Effective oxidation protection of polymer micelles for copper nanoparticles in water, *RSC Adv.* 4:14193-14196. DOI: 10.1039/C4RA00304G.
- Mu Xin and Liu Guosheng. 2014. Copper-mediated/-catalyzed fluorination reactions: new routes to aryl fluorides. *Org. Chem. Front.* DOI: 10.1039/C4QO00003J.
- Wang Zikun, Bi Xihe, Liang Yongjiu, Peiqiu Liao and Dewen Dong. 2014. A copper-catalyzed formal O-H insertion reaction of α -diazo-1,3-dicarbonyl compounds to carboxylic acids with the assistance of isocyanide, *Chem. Commun.* 50:3976-3978. DOI: 10.1039/C4CC00402G.
- Wenn Benjamin, Conradi Matthias, Andre Demetrio Carreiras, David M. Haddleton and Thomas Junkers. 2014. Photo-induced copper-mediated polymerization of methyl acrylate in continuous flow reactors. *Polym. Chem.* 5:3053-3060. DOI: 10.1039/C3PY01762A.
- Peng shusen, Zeng Zhixiang, Wenjie Zhao, He Li, Jianmin Chen, Jin Han and xuedong Wu. 2014. Novel functional hybrid silica sol-gel coating for copper protection via in situ thiol-ene click reaction. *RSC Adv.* DOI: 10.1039/C4RA00142G.
- Rogan Luke, Hughes N Louise, Cao Qun, Laura M. Dornan and Mark J. Muldoon. 2014. Copper(I)/ketoABNO Catalysed Aerobic Alcohol Oxidation, *Catal. Sci. Technol.* DOI: 10.1039/C4CY00219A.
- Hui Alice Kay, Lord Richard L and Caulton Kenneth G. 2014 In Search of Redox Noninnocence between a Tetrazine Pincer Ligand and Monovalent Copper, *Dalton Trans.* DOI: 10.1039/C3DT52490F.
- CHEN SHEN-MING, Palanisamy Selvakumar, Chelladurai Karupiah, Cheng-Yu Yang and Prakash Periakaruppan, Simultaneous and selective electrochemical determination of dihydroxybenzene isomers at reduced graphene oxide and copper nanoparticles composite modified glassy carbon electrode, *Anal. Methods*, 2014; DOI: 10.1039/C4AY00433G.
- Régis Tadeu Santiago, Tiago Quevedo Teodoro and Roberto Luiz Andrade Haiduke, The Nuclear Electric Quadrupole Moment of Copper, *Phys. Chem. Chem. Phys.*, 2014; DOI: 10.1039/C4CP00706A.
- Aillerie Alexandre, Pellegrini Sylvain, Till Bousquet and Lydie Pélineski, *In situ* generation of ammonia for the copper-catalyzed synthesis of primary aminoquinolines, *New J. Chem.*, 2014,38, 1389-1391 DOI: 10.1039/C4NJ00046C.
- Deka Pangkita, Deka Ramesh C. and Pankaj Bharali, *In situ* generated copper nanoparticle catalyzed reduction of 4-nitrophenol, *New J. Chem.*, 2014,38, 1789-1793 DOI: 10.1039/C3NJ01589K.
- witlicka-Olszewska Anna, Machura Barbara, Jerzy Mrozi ski, Bo ena Kali ska, Rafał Kruszynski and Mateusz Penkala, Effect of N-donor ancillary ligands on structural and magnetic properties of oxalate copper(II) complexes, *New J. Chem.*, 2014,38, 1611-1626 DOI: 10.1039/C3NJ01541F.
- Li Shengliang, Cao Weipeng, Anil Kumar, Shubin Jin, Yuanyuan Zhao, Chunqiu Zhang, Guozhang Zou, Paul C. Wang, Feng Li and Xing-Jie Liang, Highly sensitive simultaneous detection of mercury and copper ions by ultrasmall fluorescent DNA-Ag nanoclusters, *New J. Chem.*, 2014,38, 1546-1550 DOI: 10.1039/C3NJ01019H.
- Huh Jae-Hoon, Kim Seung Hyun, Jae Hwan Chu, Sung Youb Kim, Ji Hyun Kim and Soon-Yong Kwon, Enhancement of seawater corrosion resistance in copper using acetone-derived graphene coating, *Nanoscale*, 2014; DOI: 10.1039/C3NR05997A.
- Suchand B., Krishna J., Mritunjoy K. and G. Satyanarayana, Lewis acid promoted C-C and

- copper-catalyzed C–O bond formation: synthesis of neoflavans, *RSC Adv.*, 2014,4, 13941-13945, DOI: 10.1039/C4RA00048J.
- Shekarrao Kommuri, Kaishap Partha Pratim, Gogoi Sanjib and Boruah Romesh C., Efficient synthesis of isoquinolines and pyridines *via* copper(I)-catalyzed multi-component reaction, *RSC Adv.*, 2014,4, 14013-14023 DOI: 10.1039/C3RA46722H.
- Kali Venkata, Srirapu Vara Prasad, Sharma Chandra Shekhar, Rahul Awasthi, Ravindra Nath Singh and Akhoury Sudhir Kumar Sinha, Copper–iron–molybdenum mixed oxides as efficient oxygen evolution electrocatalysts, *Phys. Chem. Chem. Phys.*, 2014; DOI: 10.1039/C3CP55453H.
- Koo Youngmi, Yun Yeoheung, Rachit Malik, Leon White, Boyce Collins, Jagannathan Sankar, Noe T Alvarez, Vesselin N Shanov and Mark J Schulz, Aligned Carbon Nanotube/Copper Sheets: A New Electrocatalyst for CO₂ Reduction to Hydrocarbons, *RSC Adv.*, 2014; DOI: 10.1039/C4RA00618F.
- Gonzalez-Posada Fernando, R. Sellappan, Bert Vanpoucke and Dinko Chakarov, Oxidation of copper nanoparticles in water monitored *in situ* by localized surface plasmon resonance spectroscopy, *RSC Adv.*, 2014, DOI: 10.1039/C3RA47473A,
- Yang Yuwen, Zhang-Hui Lu, Yujuan Hu, Zhujun Zhang, Weimei Shi, Xiangshu Chen and Tingting Wang, Facile *in situ* synthesis of copper nanoparticles supported on reduced graphene oxide for hydrolytic dehydrogenation of ammonia borane, *RSC Adv.*, 2014,4, 13749-13752 DOI: 10.1039/C3RA47023G.
- Wang Yifeng and Haiyan Zhu, Detection of PFOS and copper (II) ions based on complexation induced fluorescence quenching of porphyrin molecules, *Anal. Methods*, 2014,6, 2379-2383 DOI: 10.1039/C3AY41902A.
- Dantas L. M. F., P. S. Castro, R. C. Peña and M. Bertotti, Amperometric determination of hydrogen peroxide using a copper microelectrode, *Anal. Methods*, 2014, 6, 2112-2116 DOI: 10.1039/C3AY41980K.
- Li Zonghao, Chen Jiaxi, Mousheng Liu and Yaling Yang, Supramolecular solvent-based microextraction of copper and lead in water samples prior to reacting with synthesized Schiff base by flame atomic absorption spectrometry determination, *Anal. Methods*, 2014,6, 2294-2298, DOI: 10.1039/C3AY00065F.
- Pourreza Nahid and Golmohammadi Hamed, Colorimetric sensing of copper based on its suppressive effect on cloud point extraction of label free silver nanoparticles, *Anal. Methods*, 2014,6, 2150-2156 DOI: 10.1039/C3AY42149J.
- Heard Christopher J. and Johnston Roy L., A theoretical study of the structures and optical spectra of helical copper–silver clusters, *Phys. Chem. Chem. Phys.*, 2014; DOI: 10.1039/C3CP55507K.
- Kitchen Jonathan A., Martinho Paulo N., Grace G. Morgan and Thorfinnur Gunnlaugsson, Synthesis, crystal structure and EPR spectroscopic analysis of novel copper complexes formed from *N*-pyridyl-4-nitro-1,8-naphthalimide ligands, *Dalton Trans.*, 2014; DOI: 10.1039/C3DT53323A,
- Chang Shu-Hao, Chiu Bo-Cheng, Tzu-Lun Gao, Shao-Lou Jheng and Hsing-Yu Tuan, Selective synthesis of copper gallium sulfide (CuGaS₂) nanostructures of different sizes, crystal phases, and morphologies, *CrystEngComm*, 2014; DOI: 10.1039/C3CE42530D.
- Zhou Wen, Wang Xiaoyong, Ming Hu, Chengcheng Zhu and Zijian Guo, A mitochondrion-targeting copper complex exhibits potent cytotoxicity against cisplatin-resistant tumor cells through a multiple mechanism of action, *Chem. Sci.*, 2014; DOI: 10.1039/C4SC00384E.
- Wang Wei, Leng Fei, Lei Zhan, Yong Chang, Xiao Xi Yang, Jing Lan and Cheng Zhi Huang, One-step prepared fluorescent copper nanoclusters for reversible pH-sensing, *Analyst*, 2014; DOI: 10.1039/C4AN00113C.
- Wu Fei, Myung Yoon and Parag Banerjee, Unravelling transient phases during thermal oxidation of copper for dense CuO nanowire growth, *CrystEngComm*, 2014; DOI: 10.1039/C4CE00275J.
- Wang Huijie, Yu Jing, Yizhi Wu, Weijia Shao and Xiaoliang Xu, A facile two-step approach to prepare superhydrophobic surfaces on copper substrates, *J. Mater. Chem. A*, 2014,2, 5010-5017, DOI: 10.1039/C3TA15102F.
- Fairbairn Robyn E., McLellan Ross, Ruaraidh D. McIntosh, Maria A. Palacios, Euan K. Brechin and Scott J. Dalgarno, Oxalix[4]arene-supported di-, tetra- and undecanuclear copper(II) clusters, *Dalton Trans.*, 2014; 43, 5292-5298, DOI: 10.1039/C3DT53088D.
- Khemnar Ashok B. and Bhanage Bhalchandra M., Copper catalyzed nitrile synthesis from aryl halides using formamide as a nitrile source, *RSC Adv.*, 2014,4, 13405-13408 DOI: 10.1039/C3RA48075E.
- Giacovazzi Roberto, Ciofini Ilaria, Li Rao, Christian Amatore and Carlo Adamo, Copper–amyloid- complex may catalyze peroxynitrite production in brain: evidence from molecular modeling, *Phys. Chem. Chem. Phys.*, 2014; DOI: 10.1039/C3CP54839B.
- Kato Masako, Ohba Tadashi, Atsushi Kobayashi, Ho-Chol Chang and Tatsuhisa Kato, Hysteretic vapour response of a

- heterodinuclear platinum(II)-copper(II) complex derived from the dimer-of-dimer motif and guest-absorbing site, *Dalton Trans.*, 2014; DOI: 10.1039/C4DT00316K.
- Chen Hongxia, Zhang Jiangjiang, Xinjian Liu, Yanmin Gao, Zonghuang Ye and Genxi Li, Colorimetric copper(II) ion sensor based on the conformational change of peptide immobilized onto the surface of gold nanoparticles, *Anal. Methods*, 2014; DOI: 10.1039/C3AY42211A.
- Letko Christopher S., Rauchfuss Thomas B., Zhou Xiaoyuan, and Gray Danielle L. Influence of Second Coordination Sphere Hydroxyl Groups on the Reactivity of Copper (I) Complexes, *Inorg. Chem.*, 2012, 51 (8), pp 4511–4520, Publication Date (Web): March 27, 2012, DOI: 10.1021/ic202207e.
- Potapov Alexey, Lancaster Kyle M., Richards John H., Gray Harry B., and Goldfarb Daniella, Spin Delocalization Over Type Zero Copper *Inorg. Chem.*, 2012, 51 (7), pp 4066–4075, Publication Date (Web): March 20, 2012 DOI: 10.1021/ic202336m.
- Guha Pampa M., Phan Hoa, Kinyon Jared S., Brotherton Wendy S., Sreenath Kesavapillai, Simmons J. Tyler, Wang Zhenxing, Clark Ronald J., Dalal Naresh S., Shatruck Michael, and Lei Zhu, Structurally Diverse Copper(II) Complexes of Polyaza Ligands Containing 1,2,3-Triazoles: Site Selectivity and Magnetic Properties. *Inorg. Chem.*, 2012, 51 (6), pp 3465–3477, Publication Date (Web): March 7, 2012 DOI: 10.1021/ic2021319.
- Prabhakaran Rathinasabapathi, Kalaivani Palaniappan, Renukadevi Somanur V., Huang Rui, Senthilkumar Kittusamy, Karvembu Ramasamy, and Natarajan Karuppanan, Copper Ion Mediated Selective Cleavage of C–S Bond in Ferrocenylthiosemicarbazone Forming Mixed Geometrical [(PPh₃)Cu(μ-S)₂Cu(PPh₃)₂] Having Cu₂S₂ Core: Toward a New Avenue in Copper–Sulfur Chemistry *Inorg. Chem.*, 2012, 51 (6), pp 3525–3532, Publication Date (Web): February 29, 2012 DOI: 10.1021/ic2022616.
- Kozlev ar Bojan, Kitanovski Nives, Jagli i Zvonko, Bandeira Nuno A. G., Robert Vincent, Guennic Boris Le, and Gamez Patrick, Cis–Trans Isomeric and Polymorphic Effects on the Magnetic Properties of Water-Bridged Copper Coordination Chains *Inorg. Chem.*, 2012, 51 (5), pp 3094–3102, Publication Date (Web): February 22, 2012 DOI: 10.1021/ic202568y.
- Comba Peter, Haaf Christina, Helmle Stefan, Karlin Kenneth D., Pandian Shanthi, and Arkadius Waleska Dioxygen Reactivity of New Bispidine–Copper Complexes *Inorg. Chem.*, 2012, 51 (5), pp 2841–2851, Publication Date (Web): February 14, 2012 DOI: 10.1021/ic2019296.
- Zhang Xiaolin, Jing Xu, Liu Tao, Han Gang, Huaqiang Li, and Chunying Duan Dual-Functional Gadolinium-Based Copper(II) Probe for Selective Magnetic Resonance Imaging and Fluorescence Sensing *Inorg. Chem.*, 2012, 51 (4), pp 2325–2331, Publication Date (Web): February 8, 2012 DOI: 10.1021/ic202322f.
- Osório Renata E. H. M. B., Peralta Rosely A., Bortoluzzi Adailton J., Almeida Vicente R. de, Szpoganicz Bruno, Fischer Franciele L., Terenzi Hernán, Antonio S. Mangrich, Karen Mary Mantovani, Dalva E. C. Ferreira, Willian R. Rocha, Wolfgang Haase, Zbigniew Tomkowicz, Ademir dos Anjos, and Ademir Neves Synthesis, Magnetostructural Correlation, and Catalytic Promiscuity of Unsymmetric Dinuclear Copper(II) Complexes: Models for Catechol Oxidases and Hydrolases. *Inorg. Chem.*, 2012, 51 (3), pp 1569–1589, Publication Date (Web): January 19, 2012 DOI: 10.1021/ic201876k.
- Nagy Nóra V., Doorslaer Sabine Van, Szabó-Plánka Terézia, Rompaey Senne Van, Andrea Hamza, Ferenc Fülöp, Gábor K. Tóth, and Antal Rockenbauer Copper(II)-Binding Ability of Stereoisomeric cis- and trans-2-Aminocyclohexanecarboxylic Acid–l-Phenylalanine Dipeptides. A Combined CW/Pulsed EPR and DFT Study *Inorg. Chem.*, 2012, 51 (3), pp 1386–1399, Publication Date (Web): January 6, 2012, DOI: 10.1021/ic2016116.
- Reger Daniel L., Debreczeni Agota, and Smith Mark D., Jezierska Julia, Ozarowski Andrew, Copper(II) Carboxylate Dimers Prepared from Ligands Designed to Form a Robust ... Stacking Synthron: Supramolecular Structures and Molecular Properties *Inorg. Chem.*, 2012, 51 (2), pp 1068–1083, Publication Date (Web): December 27, 2011 DOI: 10.1021/ic202198k.
- Tjioe Linda, Joshi Tanmaya, Forsyth Craig M., Moubaraki Boujemaa, Keith S. Murray, Joël Brugger, Bim Graham, and Leone Spiccia Phosphodiester Cleavage Properties of Copper(II) Complexes of 1,4,7-Triazacyclononane Ligands Bearing Single Alkyl Guanidine Pendants *Inorg. Chem.*, 2012, 51 (2), pp 939–953, Publication Date (Web): December 22, 2011 DOI: 10.1021/ic2019814.
- Mendola Diego La, Farkas Daniel, Bellia Francesco, Magrì Antonio, Travaglia Alessio, Örjan Hansson, and Enrico Rizzarelli Probing the Copper(II) Binding Features of Angiogenin. Similarities and Differences between a N-Terminus Peptide Fragment and the Recombinant Human Protein *Inorg. Chem.*, 2012, 51 (1), pp 128–141, Publication Date (Web): December 7, 2011, DOI: 10.1021/ic201300e.

- Turba Sabrina, Foxon Simon P., Beitat Alexander, Heinemann Frank W., Konstantin Petukhov, Paul Müller, Olaf Walter, Francesc Lloret, Miguel Julve, and Siegfried Schindler Syntheses, Characterization, and Magnetic Studies of Copper(II) Complexes with the Ligand N,N,N,N -Tetrakis(2-pyridylmethyl)-1,3-benzenediamine (1,3-tpbd) and its Phenol Derivative 2,6-Bis[bis(2-pyridylmethyl)amino]-p-cresol] (2,6-Htpcd) *Inorg. Chem.*, 2012, 51 (1), pp 88–97 Publication Date (Web): December 6, 2011 DOI: 10.1021/ic201051g.
- Nuss Gernot, Saischek Gerald, Harum Bastian N., Volpe Manuel, Ferdinand Belaj, and Nadia C. Mösch-Zanetti Pyridazine Based Scorpionate Ligand in a Copper Boratrane Compound *Inorg. Chem.*, 2011, 50 (24), pp 12632–12640 Publication Date (Web): November 17, 2011, DOI: 10.1021/ic201666w.
- Kalita Apurba, Kumar Pankaj, Deka Ramesh C., and Mondal Biplab, Role of Ligand to Control the Mechanism of Nitric Oxide Reduction of Copper(II) Complexes and Ligand Nitrosation *Inorg. Chem.*, 2011, 50 (23), pp 11868–11876 Publication Date (Web): October 31, 2011, DOI: 10.1021/ic201582w.
- Miller Kayla M., McCullough Shannon M., Lepekhina Elena A., Thibau Isabelle J., and Robert D. Pike , Xiaobo Li, James P. Killarney, and Howard H. Patterson Copper(I) Thiocyanate-Amine Networks: Synthesis, Structure, and Luminescence Behavior., *Inorg. Chem.*, 2011, 50 (15), pp 7239–7249, Publication Date (Web): July 5, 2011, DOI: 10.1021/ic200821f.
- Crestani Marco G., Manbeck Gerald F., Brennessel William W., McCormick Theresa M., and Richard Eisenberg Synthesis and Characterization of Neutral Luminescent Diphosphine Pyrrole- and Indole-Aldimine Copper(I) Complexes *Inorg. Chem.*, 2011, 50 (15), pp 7172–7188, Publication Date (Web): June 29, 2011, DOI: 10.1021/ic2007588.
- Murphy amien M., Caretti Ignacio, Carter Emma, Fallis Ian A., Gobel Marcus C., James Landon, Sabine Van Doorslaer, and David J. Willock Visualizing Diastereomeric Interactions of Chiral Amine–Chiral Copper Salen Adducts by EPR Spectroscopy and DFTD *Inorg. Chem.*, 2011, 50 (15), pp 6944–6955, Publication Date (Web): June 27, 2011, DOI: 10.1021/ic200113u.
- Verma Pratik, Weir John, Mirica Liviu, and T. Daniel P. Stack Tale of a Twist: Magnetic and Optical Switching in Copper(II) Semiquinone Complexes *Inorg. Chem.*, 2011, 50 (20), pp 9816–9825, Publication Date (Web): June 22, 2011, DOI: 10.1021/ic200958g.
- Ramakrishnan Sethu, Shakthipriya Dhanasekaran, Suresh Eringathodi, Vaiyapuri Subbarayan Periasamy, Mohammad Abdulkader Akbarsha, and Mallayan Palaniandavar Ternary Dinuclear Copper(II) Complexes of a Hydroxybenzamide Ligand with Diimine Coligands: the 5,6-dmp Ligand Enhances DNA Binding and Cleavage and Induces Apoptosis *Inorg. Chem.*, 2011, 50 (14), pp 6458–6471, Publication Date (Web): June 14, 2011, DOI: 10.1021/ic1024185.
- Maurice Rémi, Sivalingam Kanthen, Ganyushin Dmitry, Guihéry Nathalie, Coen de Graaf, and Frank Neese Theoretical Determination of the Zero-Field Splitting in Copper Acetate Monohydrate *Inorg. Chem.*, 2011, 50 (13), pp 6229–6236, Publication Date (Web): June 2, 2011 DOI: 10.1021/ic200506q.